Lithosphere, published online on 6 July 2015 as doi:10.1130/L453.1

Quaternary deformation in SE Sicily: Insights into the life and cycles of forebulge fault systems

D. Di Martire[1], A. Ascione[1], D. Calcaterra[1], G. Pappalardo[2], and S. Mazzoli[1]
[1]DEPARTMENT OF EARTH SCIENCES, ENVIRONMENT AND GEO-RESOURCES, UNIVERSITY OF NAPLES FEDERICO II, 80138 Naples, ITALY
[2]DEPARTMENT OF BIOLOGICAL, GEOLOGICAL AND ENVIRONMENTAL SCIENCES, UNIVERSITY OF CATANIA, 95124 Catania, ITALY

ABSTRACT

Integrated geological, geomorphological, and differential interferometry synthetic aperture radar (DInSAR) data are used to constrain the timing and modes of activity of Quaternary fault systems in the Hyblean Plateau. This area, which represents a unique natural laboratory for studying surface deformation in relation to deep slab dynamics, has grown since middle Miocene times as a doubly plunging forebulge associated with slab rollback during NW-directed subduction. Bimodal extension has produced two mutually orthogonal normal fault systems. The detailed stratigraphic record provided by synrift sediments and postrift marine terraces allowed us to define the timing of activity of an early Pleistocene, flexure-related fault system, thus constraining the duration of a typical foreland extensional tectonic event to ~1.5 m.y. Subsequent late Quaternary to present deformation was dominated by strike-slip faulting associated with NW-oriented horizontal compression. During this latest stage, regional uplift progressively increased toward the thrust front to the NW and was accompanied by differential uplift accommodated by dip-slip components of motion along active NNW-trending faults. The general active tectonic setting of the study area, characterized by NW-oriented horizontal compression consistent with major plate convergence, and the regional uplift pattern can both be explained within the framework of intraplate shortening and foreland rebound following complete slab detachment, a major geodynamic event interpreted to have taken place at ca. 0.7 Ma in southern Italy.

LITHOSPHERE doi:10.1130/L453.1

INTRODUCTION

For decades, studies on fold-and-thrust belts all over the world have described the foreland plate sector in front of an orogen-foreland basin system as the “undeformed foreland.” Starting from the 1980s, far-field propagation of a stress field over an orogen has been assumed as an explanation of weak strain recorded in large foreland sectors ahead of the thrust front (Geiser and Engelder, 1983). Evidence for significant brittle deformation of foreland areas has been gathered during the years, and in recent times, bending of the foreland lithosphere under the weight of the growing orogen and associated forebulge development have been invoked to explain extensional faulting and fracturing in foreland sectors, a classical example being represented by the Hyblean Plateau of SE Sicily (Pedley and Grasso, 1992). Here, conjugate normal faults and fractures that form two orthogonal sets have been related to lithospheric flexure by Billi and Salvini (2003), Billi (2005), and Billi et al. (2006). The process of foreland flexuring is well known to produce outer-arc extension in the peripheral bulge and in the outermost sector of the foredeep in response to lithospheric bending (Tankard, 1986; Bradley and Kidd, 1991; Doglioni, 1995; Sinclair, 1997; Turcotte and Schubert, 2001; Langhi et al., 2011). “Tangential” (i.e., parallel to basin strike) normal faults in foredeep and forebulge settings are frequently imaged in seismic profiles (e.g., Lorenzo et al., 1998; Matenco and Bertotti, 2000; Mazzoli et al., 2001, 2008; Ranero et al., 2003; Shiner et al., 2004). These structures, which show dominant forelandward, but also hinterlandward, dips (e.g., Maillard et al., 1992; Scisciani et al., 2001; Krzywiec, 2001; Tavarnelli and Peacock, 2002; Bolis et al., 2003; Tinterri and Muzzi Magalhaes, 2011), form half-grabens, grabens, and horsts that substantially control the distribution and accumulation of foredeep deposits (e.g., Casnedi, 1988; Tinterri and Muzzi Magalhaes, 2011).

Transversal extensional deformation structures, oriented perpendicular to “tangential” ones, can also form during flexure (e.g., Destro, 1995; Medwedeff and Krantz, 2002; Quintà and Tavani, 2012). “Radial” (i.e., normal to basin strike) normal faults form due to the arcuate shape of the foredeep, inducing arc-parallel stretching (e.g., Doglioni, 1995). The amount of along-strike foredeep stretching increases with orogen curvature (e.g., Zhao and Jacobi, 1997; Whitaker and Engelder, 2006), as it derives from the sum of cross-sectional and along-strike curvature.

Foredeep extensional structures, particularly “tangential” faults and associated basin depocenters and structural highs, are well known to play a key role in subsequent tectonic processes associated with thrust propagation into the foredeep (e.g., Butler, 1989; Scisciani et al., 2001; Mazzoli et al., 2002; Tavarnelli and Peacock, 2002). Increasing evidence suggests that these features represent very important, widespread background structures in rocks later involved in fold-and-thrust belts (Calamita and Deiana, 1980; Scisciani et al., 2001; Lash and Engelder, 2007; Casini et al., 2011; Beaudoin et al., 2012; Quintà and Tavani, 2012; Tavani et al., 2012). For example, foreland flexure–related inherited fracture networks, being independent of structural position within folds, likely play an important role for fluid flow, e.g., in fractured carbonate reservoirs (Vitale et al., 2012).

The peculiar foreland continental sector represented by the African plate indentor of SE Sicily (e.g., Yellin-Dror et al., 1997), located in front of a recess and partly surrounded by two salients of the orogen (Fig. 1), is characterized by vigorous tectonic activity beyond that expected by the relatively simple foreland flexuring processes described here.

In this paper, we discuss well-exposed fault systems in the Augusta area, in the eastern portion of the Hyblean Plateau. The sedimentary and geomorphological record is well preserved in this area and provides detailed stratigraphic constraints on the onset and end of activity of various Quaternary fault systems. These fault

Lithosphere, published online on 6 July 2015 as doi:10.1130/L453.1

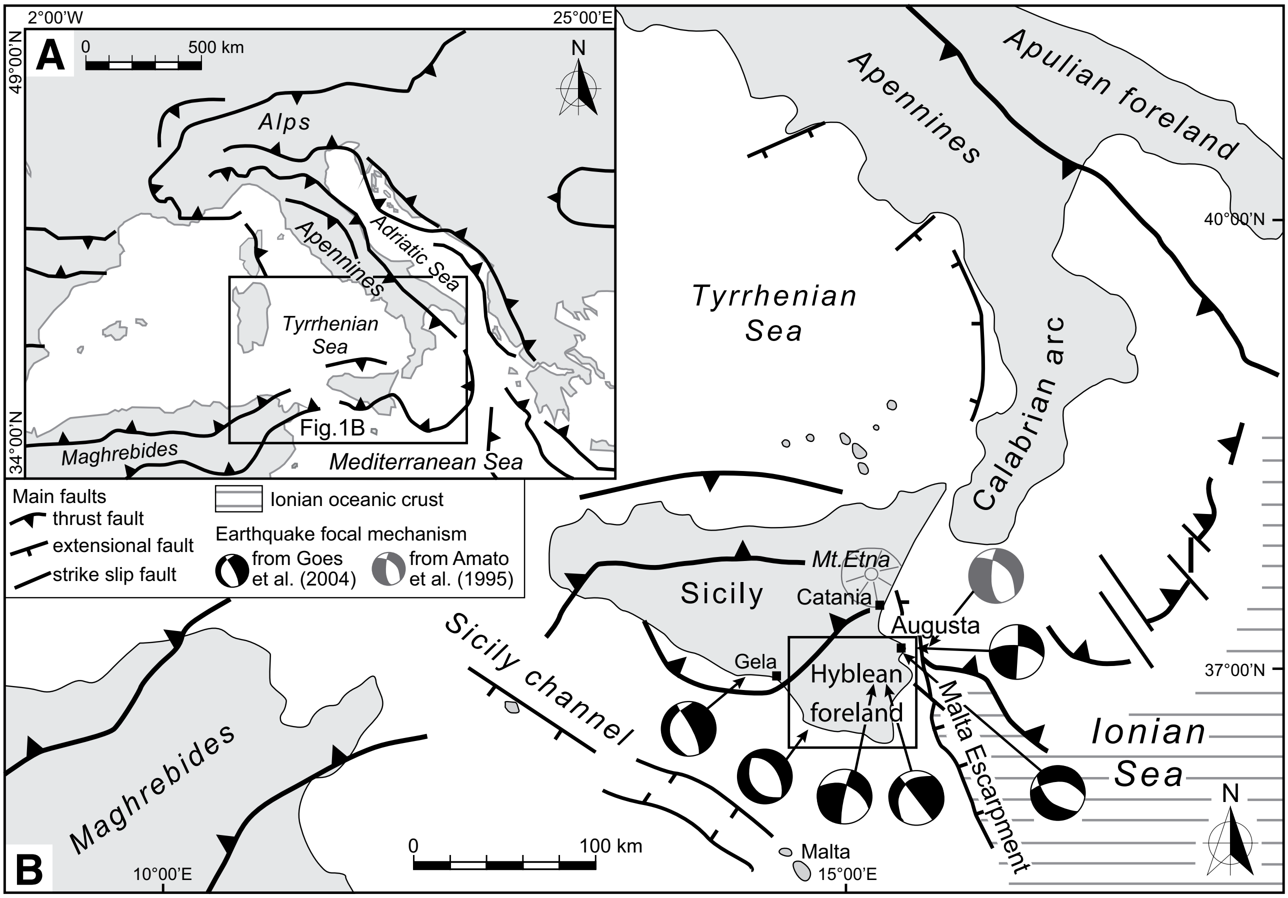

Figure 1. (A) Tectonic sketch map of the central Mediterranean region, showing main fold-and-thrust belts. (B) Tectonic sketch map of Sicily and surrounding areas, showing epicenter locations and focal mechanisms of shallow earthquakes (≤25 km deep) that occurred between 1997 and 2002; the box indicates location of the map in Figure 2 (redrawn and modified after Billi et al., 2006).

systems show different trends and kinematics, as well as cumulative displacements on the order of hundreds of meters to kilometers. We particularly focus on an early Pleistocene faulting event that controlled the deposition of a thick carbonate-clastic succession. The detailed stratigraphic record provided by synrift sediments and postrift marine terraces allows us to define the timing of activity of related fault systems, thereby constraining the complete duration of a typical extensional tectonic event affecting a foreland area. As this area is still tectonically active, we also used multitemporal interferometry (differential interferometry synthetic aperture radar [DInSAR]) analysis to unravel the behavior of the late Quaternary fault system that controls the seismotectonic setting of SE Sicily. However, since high-rate vertical motions involving subsidence phenomena on short time scales—comparable to those recorded by radar techniques—may be induced by significant water-level decline due to large-volume groundwater pumping, available hydrogeological information has also been taken into account.

The features analyzed in this study provide clear evidence of the complexity and relevance of foreland structures, well beyond the traditional notions of far-field foreland stress or bending-related brittle deformation of forebulge sectors. In particular, the relationships between surface deformation and deep geodynamic processes (i.e., slab rollback vs. slab breakoff) are emphasized. These results have important implications for a better understanding of tectonic processes—including active faulting and seismogenesis—in foreland areas, which provide further insights into the widespread occurrence and important role of inherited prethrusting structures in fold-and-thrust belt evolution (e.g., Butler, 1989).

METHODS

This study was carried out through a combined approach that integrates topography analysis, DInSAR analysis, and field controls with hydrogeological information.

The hydrogeological information was used to reconstruct the groundwater surface and flow orientations of the main aquifer in the Augusta basin.

The geomorphological analysis was carried out through the analysis of topographic maps from the Italian Istituto Geografico Militare (IGM 1:25,000 scale maps), and Regione Sicilia (Carta Tecnica Regionale 1:10,000 scale maps). The geomorphological analysis is aimed at identifying and further constraining late Quaternary differential vertical motions, taking into account the poor constraints on recent fault activity provided by stratigraphy alone. In particular, we focused on crosscutting relationships between the main faults and the wave-cut/wave-built marine terraces. Keys to the identification of vertical offsets that postdate terrace formation are the spatial distribution, and shape, of the marine terraces, and alignments of straight scarps with straight valleys or valley trunks that affect the terraced surfaces.

The DInSAR technique is able to detect displacements that occur between subsequent radar acquisitions in the sensor-target direction (line of sight [LOS]) with subcentimetric precision.

Lithosphere, published online on 6 July 2015 as doi:10.1130/L453.1

In the surface deformation detection field, the DInSAR technique allows one to obtain spatially and temporally dense measurements over large areas (from 5 km × 5 km to 100 km × 100 km). In addition, the availability of a now several-decades-long (since 1992) image archive allows us to reconstruct the history and evolution of previously unmonitored phenomena. Over the past 20 yr, synthetic aperture radar (SAR) technology has greatly improved, and many satellite constellations have been launched: ERS1/2 and ENVISTAT ASAR (European Space Agency), JERS-1 SAR (Japanese Aerospace Exploration Agency), RADARSAT-1/2 (Canadian Space Agency), TerraSAR-X and TanDEM-X (Infoterra, Germany), COSMO-SKYMed (Italian Space Agency), and SENTINEL (European Space Agency). The development of SAR technology has allowed the implementation of image-processing algorithms that produce increasingly reliable velocity maps and temporal series of deformation. Two main groups of algorithms may be distinguished: algorithms that work at "full resolution" (i.e., 4 × 20 m for medium-resolution SAR images or 3 × 3 m for high-resolution SAR images), which consider only those points characterized by radar backscattering signal (phase) stable in time, called persistent scatterer (PS) algorithms (Ferretti et al., 2000; Werner et al., 2003; Arnaud et al., 2003; Hooper et al., 2004; Duro et al., 2005; Costantini et al., 2008; Iglesias et al., 2014), and those working at "medium resolution" (usually at 60 × 60 m for medium-resolution SAR images or ~10 × 10 m for high-resolution SAR images), which evaluate the coherence value. The latter, as reported in Seymour and Cumming (1994), represents the maximum likelihood estimator of the phase quality over an estimation window (also called multilook). This technique is named small baselines subset (SBAS), or coherence-based (Berardino et al., 2002; Mora et al., 2003; Lanari et al., 2004; Prati et al., 2010; Sowter et al., 2013). In recent years, algorithms that incorporate both the PS and SBAS approaches have been proposed (Hooper, 2008; Ferretti et al., 2011).

The DInSAR technique is based on the computation of interferometric phase differences (δϕint) for each pixel, constituting the interferogram, between two SAR images acquired in different spatial positions (spatial baseline) with a difference of time (temporal baseline) using the following formula (Hanssen, 2001):

$$\delta\phi\,\mathrm{int} = \delta\phi\mathrm{flat} + \delta\phi\mathrm{topo} + \delta\phi\mathrm{displ} + \delta\phi\mathrm{atm} + \delta\phi\mathrm{noise}, \qquad (1)$$

where δϕflat is the flat Earth component related to range distance in absence of topography; δϕtopo is the topographic phase; δϕdispl is the component due to the displacement of the terrain in the LOS direction (line that goes from the radar to the observed point) between the SAR acquisitions; δϕatm is the phase related to atmospheric artifacts; and δϕnoise accounts for degradation factors related to temporal decorrelation. It is worth pointing out that the δϕflat, δϕtopo, and δϕatm terms can be removed because the orbital and topographical parameters are known. In particular, as far as δϕtopo concerns, if a digital terrain model (DTM) with an adequate resolution is available, the contribution of known topography can be almost completely removed from the interferometric phase, δφint, such as to detect the ground motions in the so-called differential interferogram.

In this study, DInSAR was performed by means of a SUBSOFT processor, based on the coherent pixels technique algorithm (CPT; Mora et al., 2003; Blanco-Sánchez et al., 2008; Iglesias et al., 2014) developed by the researchers of the Remote Sensing Laboratory (RSLab) of the Universitat Politecnica de Catalunya (UPC). We use Environmental Satellite–Advanced Synthetic Aperture Radar (ENVISAT-ASAR) images spanning the time period 2003–2010. In detail, the data sets consist of 45 and 50 single look complex (SLC) images in ascending and descending orbit, respectively, acquired between June 2004 and July 2010, and April 2003 and June 2010.

The interferometric chain implemented in the SUBSOFT processor is reported in the Appendix.

GEOLOGICAL SETTING

The study area forms part of the Hyblean Plateau of SE Sicily (Fig. 1), which consists of a doubly plunging forebulge characterized by the occurrence of preexisting crustal heterogeneities that developed during a long-lasting tectonic evolution since Mesozoic times. The inherited crustal architecture enhanced differential retreating processes of the foreland during subsequent subduction, with the associated development of orogenic salients and recesses (Billi et al., 2006). Various generations of foreland fault systems characterized by different trends and/or kinematics have developed since middle Miocene times, which have important implications for the seismotectonic behavior of the studied area (e.g., Adam et al., 2000). This area is located within a general context encompassing the whole of Sicily and surrounding onshore and offshore areas, which are characterized by intense active tectonics witnessed by historical and recent destructive earthquakes and tsunamis, late Quaternary faulting, and fast rates of vertical and horizontal crustal motions, and quiescent as well as active volcanoes (including Etna; Billi et al., 2010, and references therein).

The Hyblean Plateau, together with the Sicily Channel and the adjacent continental shelf areas, belongs to a largely submerged portion of the African foreland domain known as the Pelagian block (Burollet et al., 1978). This block represents an indentor of the African plate during its Neogene convergence with the Eurasian plate (Caire, 1970; Bianchi et al., 1987; Butler et al., 1992), and it is characterized by crustal segmentation partly controlled by inherited structures that originated during the Mesozoic evolution of the African passive margin (Reuther et al., 1993; Robertson and Grasso, 1995). The Hyblean Plateau consists of a continental basement of unknown age, overlain by a Triassic to Quaternary sedimentary succession including dominantly carbonate sediments intercalated with Upper Triassic–Lower Jurassic, Upper Cretaceous, and Upper Miocene to Quaternary mafic volcanics (Fig. 2; Barberi et el., 1974; Patacca et al., 1979;

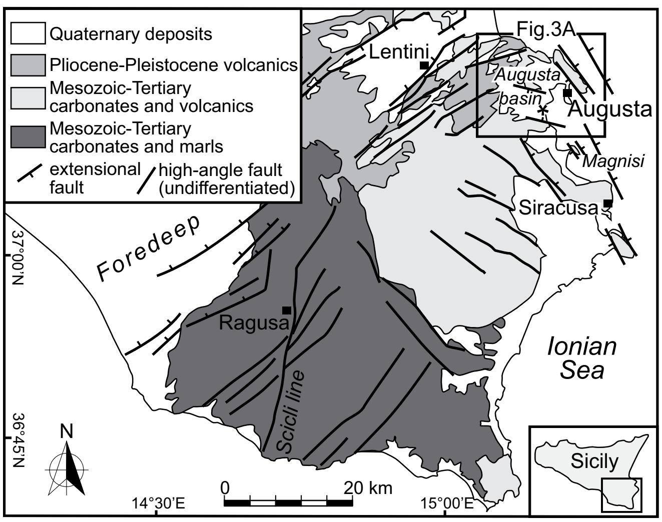

Figure 2. Geological sketch map of the Hyblean Plateau and adjacent foredeep area (modified after Billi et al., 2006; Catalano et al., 2010; Firetto Carlino et al., 2013; location in inset map and in Fig. 1B). The Quaternary deposits include the Lower Pleistocene synrift and postrift sedimentary successions, and the Middle and Upper Pleistocene deposits that blanket the marine terraces. The Augusta Basin basement successions correspond to the Mesozoic and Tertiary carbonates and volcanics. Asterisk indicates location of the Megara Hyblaea archaeological site.

Grasso et al., 1983). The whole volcano-sedimentary succession of the plateau ranges in thickness from ~5 to 6 km at its northern and eastern edges to ~10 km in its central sector (Agocs, 1959; Zarudski, 1972; Lentini, 1983; Bianchi et al., 1987; Antonelli et al., 1988). The oldest outcropping rocks consist of Cretaceous carbonates. These include both cherty-marly limestones of basin origin to the west, and platform carbonates along the Ionian margin to the east (Lentini et al., 1984). The overlying deposits include Oligocene to Miocene carbonates and marls, which represent the most abundantly outcropping units of the plateau, followed by Quaternary sediments occurring mainly along its margins (Fig. 2).

The plateau is bound to the east by the Malta Escarpment, a steep submarine slope that drops into the Ionian Sea down to a depth in excess of 3000 m (Fig. 1). The escarpment, most probably controlled by an inherited Mesozoic crustal structure (Scandone et al., 1981), may be subdivided into two different portions (Argnani and Bonazzi, 2005): The segment north of Siracusa (location in Fig. 2) is characterized by the occurrence of NNW-SSE east-dipping recent extensional faults and related sedimentary basins, whereas the segment south of Siracusa appears to not be affected by recent faulting and consists of a steep morphological surface that flattens out toward the Ionian basin. A significant change in crustal thickness occurs between the block to the west, consisting of thick continental crust extending via the Malta platform to the Maltese islands, and the thin crust of the Ionian Sea to the east.

The Hyblean Plateau is flexured to the northwest and dips below the frontal part of the Maghrebian-Sicilian fold-and-thrust belt, represented in this area by the Pliocene–Quaternary Gela Nappe. The resulting flexural basin is known as the Gela-Catania foredeep (Di Geronimo et al., 1978; Grasso et al., 1983). Magnetic and gravity data clearly outline the sharp boundaries of the Hyblean Plateau with respect to adjacent units of the African continental margin (AGIP, 1978, 1982). Bouguer anomalies are positive over the plateau, while a pronounced negative anomaly occurs west of it, where a thick pile of sediments and allochthonous thrust sheets sit on top of the flexured and downfaulted foreland carbonate succession (Grasso et al., 1990). Extensional faulting and crustal thinning are marked by significant volcanic activity during the last 8 m.y. along the northern margin of the Hyblean Plateau. This area underwent uplift associated with the formation of a broad carbonate platform on its eastern sector during the Late Tertiary (Grasso and Lentini, 1982). As a result of regional uplift, slow rates of sedimentation—or even erosion associated with local emergence—characterized the northern Hyblean area. This uplift event was coeval with slow tectonic subsidence in the western part of the Hyblean Plateau, which underwent greater rates of flexural downbending than the eastern sectors. As the Messinian sea-level fall was coeval with uplift, evaporites were only locally deposited within NE-SW-trending narrow grabens located along the northern sector of the plateau (Pedley and Grasso, 1991). Subsequent subsidence, coeval with a major early Pliocene rise in Mediterranean sea level (Butler et al., 1995), led to flooding and chalk deposition (Trubi Formation). These new conditions created the accommodation space for Pliocene–Pleistocene sediment accumulation within the Gela-Catania foredeep, a foreland basin filled with several hundred meters of marine clays and sands unconformably overlying older volcano-sedimentary successions. Following a massive late Miocene–early Pleistocene basaltic volcanic flare-up (Schmincke et al., 1997), renewed uplift characterized the Hyblean Plateau during the middle to late Pleistocene, coeval with the end of thrusting along the frontal part of the Sicilian-Maghrebian fold-and-thrust belt. This renewed uplift is inferred from the occurrence of Lower Pleistocene shallow-water sediments at elevations in excess of 600 m in the northwestern part of the plateau (Schmincke et al., 1997), and from uplifted marine terraces developed along the whole coastal area of southeastern Sicily. Based on marine terrace elevations, uplift rate values of ~2 mm/yr in the north (Taormina area), decreasing southward, have been estimated (Carbone et al., 1982a; Westaway, 1993; Bianca et al., 1999; Bordoni and Valensise, 1998; Monaco et al., 2002; Di Stefano and Branca, 2002; Antonioli et al., 2003, 2006, 2009; Catalano and De Guidi, 2003; Ferranti et al., 2006; Catalano et al., 2008, 2010; Lambeck et al., 2011). However, recent studies (e.g., Scicchitano et al., 2008) suggest that the area is undergoing differential displacements upon a regional, long-term uplift process.

Fault Systems and Seismotectonic Setting of the Hyblean Plateau

The main fault trends of the study area, outlined by Carbone et al. (1982b), include: (1) an older, inactive, NW-SE–trending graben system, which was already delineated during the early Pleistocene, and the related faults of which controlled paleocoastlines; and (2) younger, NNW-SSE– and ENE-WSW–striking fault systems that, besides offsetting Quaternary deposits, also dissect the preexisting NW-SE–trending fault system. For the latter, an early Pleistocene age has been proposed by Adam et al. (2000). These authors analyzed the dominant active stress field over the study area, suggesting that earthquake faulting is mainly of strike-slip type, with a NW-SE–trending maximum compression (σ_1) and a NE-SW–oriented minimum compression (σ_3). The occurrence of active strike-slip faulting is suggested by Azzaro et al. (2000) for the so-called "Scicli Line" (Fig. 2), a major wrench fault extending for ~100 km from the Sicily Channel to the northern margin of the Hyblean Plateau. Although there is no direct evidence of activity postdating the middle Pleistocene, earthquake distribution (events in years A.D. 1698, 1818, 1895, 1949, 1980, 1990) is interpreted by the latter authors as indicating the existence of minor seismogenic sources associated with this structure. However, according to Azzaro and Barbano (2000), the main active fault system in SE Sicily is that associated with the Malta Escarpment. This fault system extends for more than 200 km from North Africa to Sicily, and controls the trend of the east coast of the island. It includes NNW-SSE–trending, dominantly extensional fault segments producing a cumulative vertical displacement of ~3000 m. The northernmost fault segment is exposed onshore in the Mount Etna area (Continisio et al., 1997; Billi et al., 2010). In the Siracusa-Augusta onshore area, clear evidence of activity of this fault system dates back to the middle Pleistocene (Carbone, 1985), while offshore seismic profiles image middle Pleistocene to Holocene faulted deposits (Hirn et al., 1997; Argnani and Bonazzi, 2005; Firetto Carlino et al., 2013). Azzaro and Barbano (2000) suggested that the Malta Escarpment fault system is the source for the large earthquakes (M ≥ 7.0) that destroyed eastern Sicily in A.D. 1169 and 1693, and also of minor events such as those of A.D. 1818 and 1848.

Although subsurface stratigraphic data suggest that the forebulge of SE Sicily grew mainly as an ENE-trending foreland monocline (Grasso and Pedley, 1990), modeling of convergent deformation in Sicily (Ben-Avraham et al., 1995) as well as structural data (Barrier, 1992; Sirovich and Pettenati, 1999; Billi et al., 2006) point to a noncylindrical, complex tectonic evolution for this foreland sector. Indeed, the structural architecture of the Hyblean Plateau is characterized by multiple sets of strike-slip and normal faults (Fig. 2) for which trends and kinematics cannot be reconciled within the framework of a single regional stress field (Adam et al., 2000). In particular, only the older NW-SE–trending normal fault systems appear to be consistent with the horizontal extension expected for the outer arc of a cylindrical forebulge (Turcotte and Schubert, 2001). Moreover, focal mechanisms of upper-crustal earthquakes recorded in the Hyblean area between 1977 and 2002 show both strike-slip and normal fault solutions (Fig. 1; Goes et al., 2004). The strike-slip solutions are consistent with the dominant kinematics of active regional faults in this area (Adam et al., 2000; Grasso et al., 2000), as well as with the NW-trending maximum shortening axis (SHmax) obtained by the analysis of borehole breakout data (Ragg et al., 1999). On the other hand, the normal fault solutions are mostly compatible with a NE-SW–oriented, horizontal maximum extension.

GEOLOGICAL SETTING OF THE AUGUSTA AREA

The Augusta Basin (Fig. 3A) is a tectonic depression, ~20 km long and 12 km wide, located in the eastern part of the Hyblean Plateau (Firetto Carlino et al., 2013). The basin is controlled by two main fault segments; namely, it is separated southward from the Magnisi–St. Panagia ridge by the NW-SE–oriented, NE-dipping Mount Climiti fault (Bianca et al., 1999; Catalano et al., 2010) and northward by the 7-km-long, NNW-SSE–trending Mount Tauro fault, which borders the Mount Tauro horst with a roughly 35-m-high scarp. From a stratigraphic point of view, the Augusta Basin is characterized by Lower Pleistocene calcarenites and sands passing upward and laterally to deep-water clays (Di Grande, 1972; Di Grande and Scamarda, 1973; Di Grande and Raimondo, 1982; Carbone, 1985; Carbone et al., 1986, 1987; I.S.P.R.A., 2011a, 2011b). These sediments rest unconformably upon an Upper Cretaceous–Miocene basement succession made of carbonates with volcanic intercalations, outcropping in the horst blocks bounding the Augusta Basin (Patacca et al., 1979; Carbone et al., 1982b, 1982c, 1986, 1987; Carbone, 1985; Bianchi et al., 1987; Dall'Antonia et al., 2001; I.S.P.R.A., 2011a). The stratigraphic gap indicates a prolonged emergence of the area during the Pliocene before tectonic collapse that led to graben formation during the late Pliocene, according to Carbone (1985), or at the onset of the Pleistocene, according to Adam et al. (2000). Younger deposits consist of widespread fossiliferous calcarenites and sands ("Panchina" Formation; Accordi, 1962) that are related to the middle Pleistocene (e.g., Accordi, 1962, 1963; Ruggieri and Greco, 1965; Carbone et al., 1982a; I.S.P.R.A., 2011b). The Panchina Formation deposits form few-meter-thick blankets on top of the wide marine terraces, which, in the Augusta area, form a flight reaching ~200 m above sea level (a.s.l.). Conversely, Upper Pleistocene shallow-marine deposits are more localized and associated with marine terraces in the coastal belts of the Mount Tauro horst and Gesira headlands (e.g., Di Grande and Scamarda, 1973; Bordonaro et al., 1984; Di Grande and Neri, 1988). The Upper Pleistocene deposits are characterized by faunal assemblages including specimens of *Strombus bubonius*, which in the Mediterranean area marks fossils associations correlated with the Last Interglacial (MIS 5) highstand (Gignoux, 1913).

Costa Mendola Area

Within the Augusta Basin, in the Costa Mendola area, an elevated ridge known as Mendola horst occurs (I.S.P.R.A., 2011a, 2011b; Fig. 3A). The Mendola Horst mainly consists of calcarenites and calcirudites of the Miocene Monti Climiti Formation. Younger deposits in contact with the Miocene carbonates include: (1) Lower Pleistocene calcarenites and shales; and (2) Middle Pleistocene veneers of calcarenites and sands of the Panchina Formation, associated with marine terraces (refer to section "Quaternary Marine Terraces and Vertical Motions of the Augusta Area"). In the northern sector of the Mendola horst, the Lower Pleistocene calcarenites rest unconformably on top of the Miocene limestones. The Lower Pleistocene shales, cropping out along the eastern flank of the Mulinello River valley, pinch out to the west and onlap the structural high. The stratigraphically overlying deposits of the Panchina Formation form discontinuous patches unconformably covering both the Lower Pleistocene calcarenites and the Miocene limestones, in both instances with the interposition—at some places—of a paleosol (I.S.P.R.A., 2011b, and references therein). Along the southern edge of the structural high, between Masseria Mendola and Balatelle (Fig. 3A), the contact between the Miocene limestones and the Lower Pleistocene shales occurs along a WNW-ESE–striking, SSW-dipping, high-angle fault. The deposits of the Panchina Formation in this area either sit stratigraphically on top of the Lower Pleistocene shales, or they are in tectonic contact with the Miocene limestones along the same high-angle fault. The highly degraded and eroded fault surface does not preserve indicators of precise fault kinematics, such as shear fibers or abrasion striae. However, it is clear from the stratigraphic separation that the fault has a significant normal dip-slip component of motion. WNW-ESE–striking, minor normal faults form a conjugate extensional set that is well exposed in Miocene limestones in the interior of the Mendola horst (Fig. 3A), roughly parallel to the main fault bounding the elevated ridge to the south.

Carbone (1985) showed how the Lower Pleistocene calcarenites represent a coarse-grained facies that is generally proximal to paleofault scarps. These deposits pass both laterally (toward the basin depocenter) and vertically to the Lower Pleistocene shales, which constitute a more distal facies and reach a thickness of several hundreds of meters in the center of fault-bounded tectonic depressions. Significant thickness variations of the Lower Pleistocene deposits along faults (e.g., the WNW-ESE–trending Costa Mendola fault; Fig. 3B) are confirmed by well log data recently provided by Firetto Carlino et al. (2013). Common synsedimentary deformation of the Lower Pleistocene calcarenites and yellow sands is mentioned by Carbone (1985).

Quaternary Marine Terraces and Vertical Motions of the Augusta Area

A flight of marine terraces and shorelines testifies to uplift coeval to Quaternary sea-level fluctuations of the Augusta area. However, the chronostratigraphic framework of marine terraces, and related uplift evaluation, is debated.

The lowest paleo–sea level indicators consist of notches carved at around 2 and 5 m a.s.l. in the Miocene carbonates of the Mount Tauro horst (I.S.P.R.A., 2011b). Higher marine terraces standing between 5 and 10 m (with inner rim around +15 m; I.S.P.R.A., 2011b) occur in the Mount Tauro and Gesira headlands. These terraces are blanketed with 1–5-m-thick Upper Pleistocene conglomerates and sands bearing *Strombus bubonius* (Di Grande and Scamarda, 1973; Bordonaro et al., 1984; Di Grande and Neri, 1988). Based on the recovery of further *Strombus*-bearing deposits, Cosentino and Gliozzi (1988; see also Bordoni and Valensise, 1998) related marine terraces at about +30–35 m in the Mount Tauro horst to the Last Interglacial. These authors estimated an uplift rate around 0.2 mm/yr since the late Pleistocene for the Mount Tauro headland. More recently, Antonioli et al. (2006) correlated the shorelines at +16 m at Mount Tauro (with a resulting 0.07 mm/yr uplift rate), and the +32 m marine terrace in the Climiti Mountains–Belvedere ridge with the 126 ka marine isotope stage (MIS) 5.5 (Lisiecki and Raymo, 2005). Marine terraces around 30 m a.s.l. at the northwestern boundary of Augusta Bay were correlated to the Last Interglacial by I.S.P.R.A. (2011a, 2011b). Higher (≥50 m a.s.l.) shorelines consist of tidal notches carved in the Climiti Mountains ridge, and large terraces generally topped by middle Pleistocene Panchina Formation deposits (I.S.P.R.A., 2011b). Collectively, six marine terraces with up to 150 m of elevation have been identified by Bianca et al. (1999) and Monaco et al. (2002). Catalano et al. (2010) distinguished 10 marine terraces, including higher subplanar, mostly erosional, surfaces resting up to 325 m a.s.l. in the uplands to the west of Augusta. These authors estimated a mean uplift rate of around 0.7 mm/yr for the last 240 k.y. (Bianca et al., 1999), and for the last 520 k.y. (Catalano et al., 2010). However, these

Lithosphere, published online on 6 July 2015 as doi:10.1130/L453.1

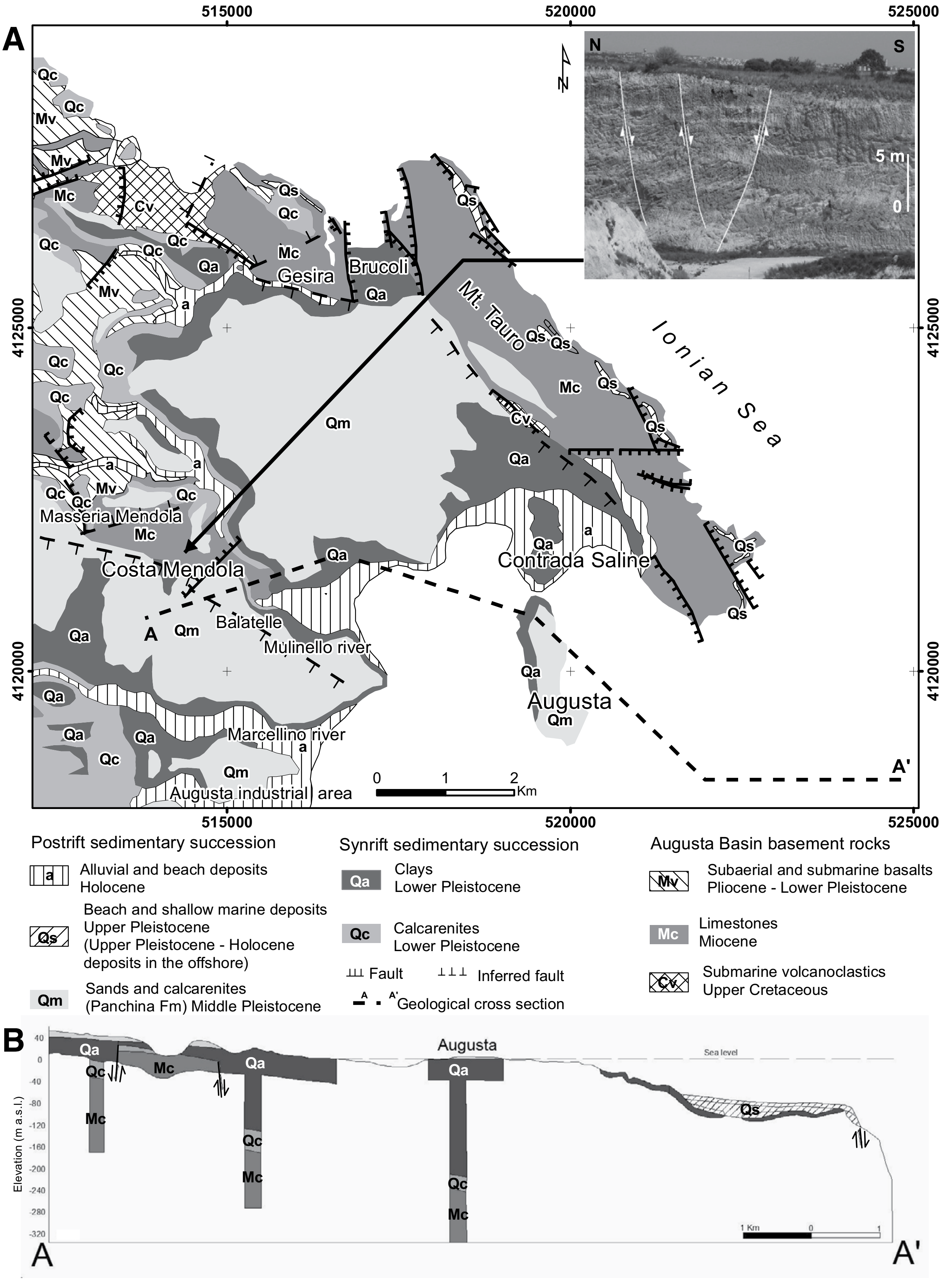

Figure 3. (A) Geological sketch map of the Augusta area (location in Fig. 2; modified after Carbone et al., 1986); inset image shows conjugate normal faults affecting Miocene limestones of the Costa Mendola horst block. (B) Onshore-offshore cross section, modified after Firetto Carlino et al. (2013) (coordinates are referred to the UTM 33N grid zone).

Lithosphere, published online on 6 July 2015 as doi:10.1130/L453.1

estimates rest on a rather questionable marine terrace chronostratigraphic framework, which is based on dating of mammal fauna from continental deposits either overlying or underlying marine deposits in the Climiti Mountains–Belvedere ridge. Within this framework, the terraces at 15 m and 105 m a.s.l. are correlated with the 60 ka MIS 3.3 and 126 ka MIS 5.5, respectively, while the occurrence of the *Strombus*-bearing deposits and notches at around +2 and +5 m in the Mount Tauro horst are neglected. The resulting mean uplift rate of ~0.7 mm/yr for the middle Pleistocene to present time span therefore appears to represent a large overestimation.

Although a large-scale southward tilting of the Hyblean Plateau during the Quaternary evolution of the forebulge area is generally recognized (see section "Geological Setting"), the Augusta area is interpreted as less uplifted with respect to the more southerly Siracusa area based on the elevation of the Last Interglacial markers and submerged Holocene markers (Ferranti et al., 2006; Antonioli et al., 2009; Lambeck et al., 2011). Based on submerged archaeological markers, Scicchitano et al. (2008) suggested that in the late Holocene, the central part of the Augusta Bay coastal belt recorded slower uplift (~0.30 mm/yr for the last 2.6 k.y. in the Megara Hyblaea site; location in Fig. 2) with respect to the morphostructural highs to the south (0.68 mm/yr for the last 3.5 k.y. in the Magnisi peninsula; location in Fig. 2).

Hydrogeological Setting of the Augusta Area

The Augusta area hosts the urban center of Augusta (the second largest town in the province of Siracusa, with ~36,000 inhabitants) and several industrial installations such as petrochemical manufacturing facilities, the activity of which started in the 1950s and was supported by the pumping of large volumes of groundwater.

The carbonate block of Mount Tauro hosts an unconfined aquifer (Mc, in Fig. 3), while the hydrogeological system of the Augusta Basin includes two carbonate aquifers. An upper, low-thickness (1–10 m) aquifer coincides with the Middle Pleistocene Panchina Formation sands and calcarenites, whereas a deeper aquifer is located in the Lower Pleistocene calcarenites and calcirudites (Qc, in Fig. 3) and the underlying Miocene carbonates (Aureli et al., 1987a, 1987b). The two aquifers are separated by an impermeable layer represented by overconsolidated Lower Pleistocene clays (Canova et al., 2012), the thickness of which ranges from a few meters to over 300 m in the offshore Augusta Bay (Carbone, 1985). Both aquifers of the Augusta Basin are in lateral contact with that of Mount Tauro along the central sector of the Mount Tauro fault. The permeability of the carbonate complexes is variable: The primary permeability ranges between 10^{-3} and 10^{-5} m/s, while the secondary permeability (favored by joints and karst caves, especially in the lower aquifer) is slightly higher, ranging from 10^{-1} to 10^{-2} m/s. Measured transmissivity ranges from 0.1 to 9×10^{-3} m^2/s.

The aquifers are exploited by deep wells (depths > 400 m) for agricultural, industrial, and potable purposes. Since the upper aquifer is characterized by low thickness, the deeper aquifer is the most exploited. The piezometric level has been affected by a progressive decline caused by overexploitation essentially by the industrial installations (I.S.P.R.A., 2011b). The groundwater surface decline started in the 1960s and increased, particularly in the coastal area, in the 1980s (I.S.P.R.A., 2011b).

The groundwater surface and flow orientations of the lower, confined aquifer have been reconstructed based on measurements dating back to 2004–2005 (Fig. 4). A comparison of the groundwater surface shown in Figure 4 with that mapped by Carbone et al. (1986) based on data dating back to 1983 points to a decline of the piezometric surface of up to 70 m in some areas. In the coastal area, such a decline caused saltwater intrusion, as documented by an official report on the 2003–2006 monitoring by the Regional Hydrographic Office (Ufficio Idrografico Regionale, 2007).

GEOMORPHOLOGICAL ANALYSIS

In the mainland area to the west of Mount Tauro, seven main marine terraces (Fig. 5) in the elevation range of ~170 m to 10–15 m a.s.l. have been identified. They are carved on variable bedrock types and generally topped by calcarenites of the Panchina Formation deposits, or younger—Upper Pleistocene—conglomerate and sands. The Upper Pleistocene terraces include the terraced surface standing at about +30 m to the NW of the Augusta peninsula (I.S.P.R.A., 2011a), and labeled t2 in Figure 5. Among such terraces, terrace t3 (standing at elevations ranging from ~50 to 60 m and rising inland up to ~65 m; Fig. 5) and the higher terrace t4 (elevation in the 90–105 m range) are carved in the Lower Pleistocene Augusta Basin deposits and in the underlying pre-Quaternary bedrock, which includes carbonates of the Mendola horst. Such relationships indicate that fault activity bounding the Mendola horst predated formation of terraces t3 and t4. Formation of terraces t3 and t4, which stand higher than—and predate—the Upper Pleistocene t2 terrace, may be related to the late part of the middle Pleistocene. The age of terraces t3 and t4 may be better constrained through correlation of the Augusta terrace flight with sea-level highstands. The correlation has been based on the sea-level curve derived by Waelbroeck et al. (2002), and the uplift rate (ranging between 0.2 and 0.3 mm/yr) inferred from elevation of the Last Interglacial shorelines in the Augusta area (e.g., Cosentino and Gliozzi, 1988; Bordoni and Valensise, 1998; Antonioli et al., 2006; Ferranti et al., 2006). Using such information, terrace t3 may be tentatively correlated with the MIS 7 highstands (with formation of its large surface mirroring successive rework-

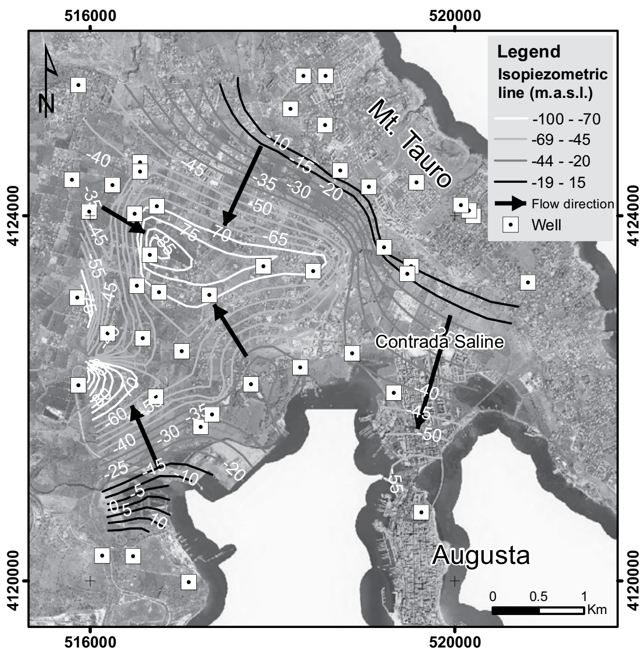

Figure 4. Groundwater surface of the carbonate confined aquifer in the Augusta Basin area; arrows indicate groundwater flow orientations; coordinates are referred to the UTM 33N grid zone.

Lithosphere, published online on 6 July 2015 as doi:10.1130/L453.1

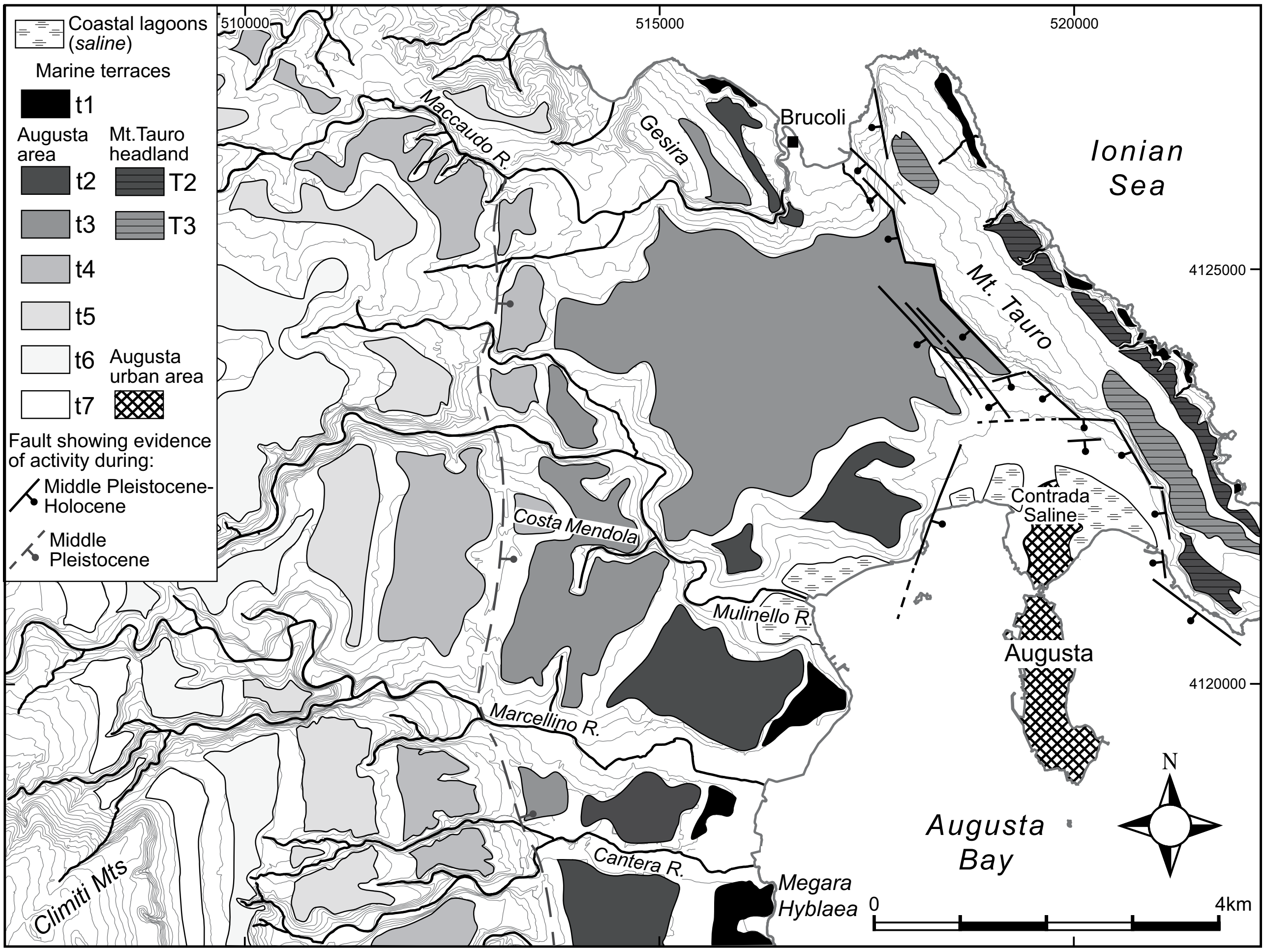

Figure 5. Quaternary marine terraces in the Augusta area (see text for chronological information), and traces of faults affecting the marine terraces (contour lines = 10 m). Coordinates are referred to the UTM 33N grid zone.

ing by the sea level in the around 200–240 ka time span), and terrace t4 can be tentatively correlated with MIS 9.3. Based on such correlation, fault activity at the Mendola horst boundaries is at least older than 330 ka.

Vertical motions along two fault systems that postdate the formation of some of the marine terraces are suggested by several pieces of evidence. One system, consisting of two main strands with a roughly N-S trend and length of ~8 km, has been identified to the west of Costa Mendola by a distinct alignment of rectilinear scarps and straight stream incisions affecting terrace t4 (Fig. 5). The activity of such structures was probably responsible for capture of the Maccaudo River (which shows a distinct change in flow orientation to the west of the fault trace; Fig. 5), and for the outline of the coastal belt perimeter. This is inferred from both the straight—roughly N-S—trend the of rims of terrace t4 compared with the more sinuous boundaries of higher terraces, and the strongly variable width of terrace t3 from the north to the south (Fig. 5).

More recent activity is recorded by the NNW-SSE–oriented Mount Tauro fault system (Fig. 5). This activity is inferred from the lack of both terraces younger than terrace t3 to the north of the Augusta peninsula, and coastal landforms carved in the fault scarp bounding the Mount Tauro fault system to the west. These observations are in contrast with evidence from the remaining Mount Tauro perimeter belt, which is characterized by bays and coastal caves raised up to 20 m a.s.l. (I.S.P.R.A., 2011b, and references therein), and marine terraces. These terraces stand around 15 m (terrace t1), 30–40 m (terrace T2), and 50 m a.s.l. (terrace T3; Fig. 5). Recent vertical motions along the Mount Tauro fault system are also suggested by deformation of terrace t3. Terrace t3 is affected by segmented rectilinear scarps oriented roughly parallel to the main Mount Tauro fault and around E-W, pointing to progressive lowering toward both the west and the southeast of the terrace surface, and by slight tilting shown by the gentle dip of such surface toward the E-SE down to 40 m. All these observations points to activity of the Mount Tauro fault system that postdate formation of both terrace t3 and the lower (Upper Pleistocene) terrace t2 (Fig. 5). More importantly, the mapped fault scarps control the perimeter of the coastal plain to the north of the Augusta peninsula, suggesting that fault activity in the forebulge area has continued until the Holocene.

MULTITEMPORAL INTERFEROMETRY SAR ANALYSIS

For the Augusta Basin area, Canova et al. (2012) discussed the results of an analysis of surface deformations obtained by the DInSAR technique using ERS (European Remote Sensing) images from years 1992–2000. Significant land subsidence in a NW-SE–trending area (including the Augusta urban area) was identified and primarily related to groundwater overexploitation.

Our DInSAR analysis is aimed at assessing the deformation trends of the area spanning from the coastline to the Costa Mendola horst to the west in the 2003–2010 time span. The first step of the analysis was the cut of a ROI (Region of Interest) of ~12 × 8 km (Fig. 6) starting from the SLC images, which cover an area of 100 × 100 km. In order to perform a fine coregistration of SAR images and to remove the topographic contribution to the interferometric phase, we used an external digital terrain model (DTM) with a 10 × 10 m resolution cell (obtained from the Tinitaly Project; Tarquini et al., 2012). In this work, a SBAS approach was used, and from the whole set of interferograms, only those with a perpendicular spatial baseline smaller than 250 m and a temporal baseline shorter than 211 d were selected. Due to the use of a multilook factor of 15 × 3 pixels (azimuth × range), the ground resolution of the outputs was resampled to 60 × 60 m. Finally, in order to both have a sufficient number of points covering the entire study area, and display a phase standard deviation of ~20° (which corresponds to a displacement standard deviation of ~1.5 mm), two coherence threshold values (0,50 and 0,40 in more than 50% of the interferograms) have been set. In total, 45 images were available for the ascending track (track 129, frame 729), and 58 interferograms were selected based on the aforementioned baseline thresholds; the mean coherence map was then constructed (Fig. 7). This map allows identification of points characterized by different stable phase quality during the time acquisition; starting from the coherence map, the next step was to identify those points with above-threshold coherence values. Such processing allows the construction of a mean velocities map (Fig. 8). The map in Figure 8 shows that the highest displacement rates (~25 mm/yr) are focused to the north of the Augusta urban area, while the area of Mount Tauro is identified as stable. Such displacement rate values are in good agreement with the results of Canova et al. (2012), based on processing of SAR data acquired in the 1992–2000 time span. It is worth nothing that both in the map of Canova et al. (2012) and in our map, the stable area (Mount Tauro horst) is separated from the unstable area (Augusta graben) by a NNW-SSE–trending lineament, which coincides with the Mount Tauro fault trace.

Fifty descending images (track 222, frame 2853) were processed. The same maximum

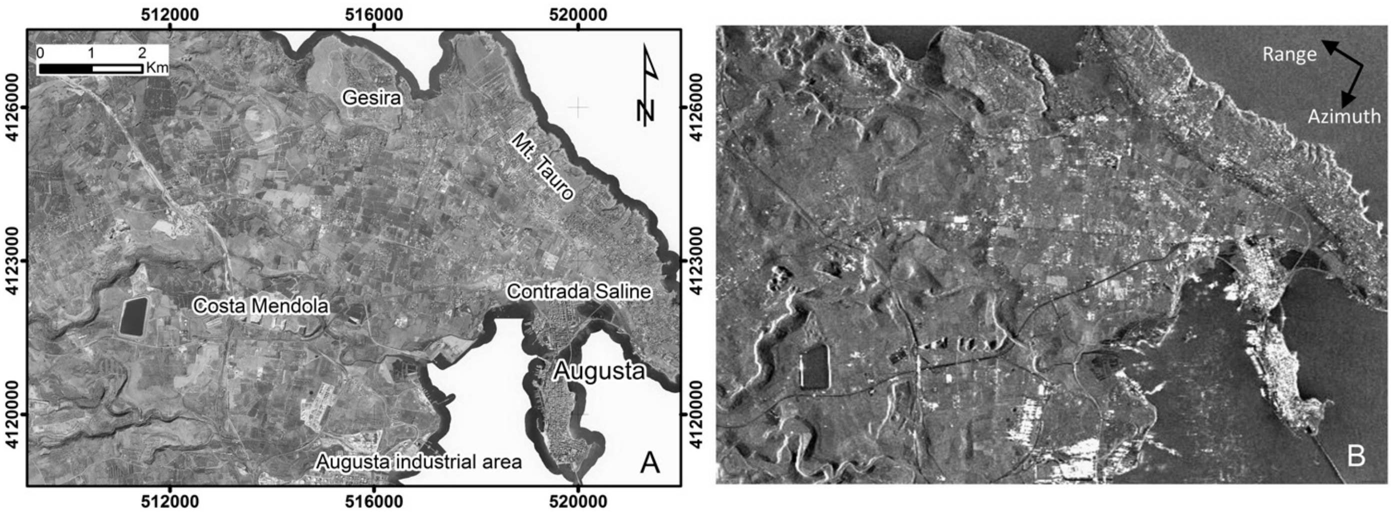

Figure 6. Coverage of the Augusta ROI (Region of Interest) (12 × 8 km). (A) Aerial photo; coordinates are referred to the UTM 33N grid zone. (B) Amplitude in dB decibel of the cropped synthetic aperture radar image acquired by the ENVISAT-ASAR mission.

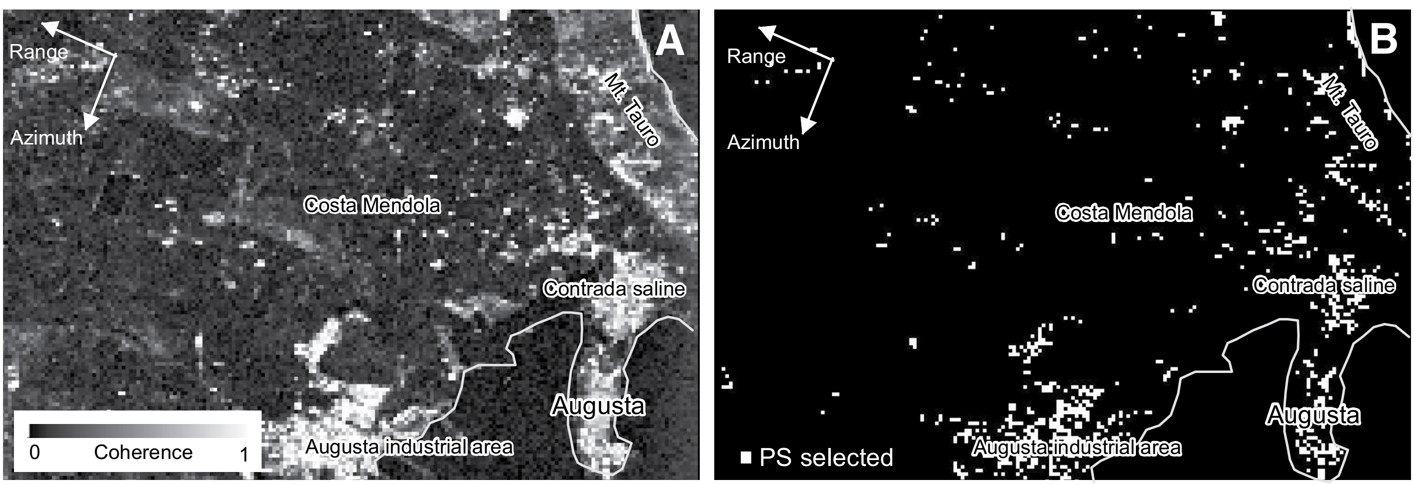

Figure 7. (A) Mean coherence map obtained from interferometric pairs with a perpendicular spatial baseline smaller than 250 m and a temporal baseline shorter than 211 d. (B) Coherent pixel selected using coherence stability method with a threshold of 0.40 in more than 50% of the interferograms. PS—persistent scatterer.

Lithosphere, published online on 6 July 2015 as doi:10.1130/L453.1

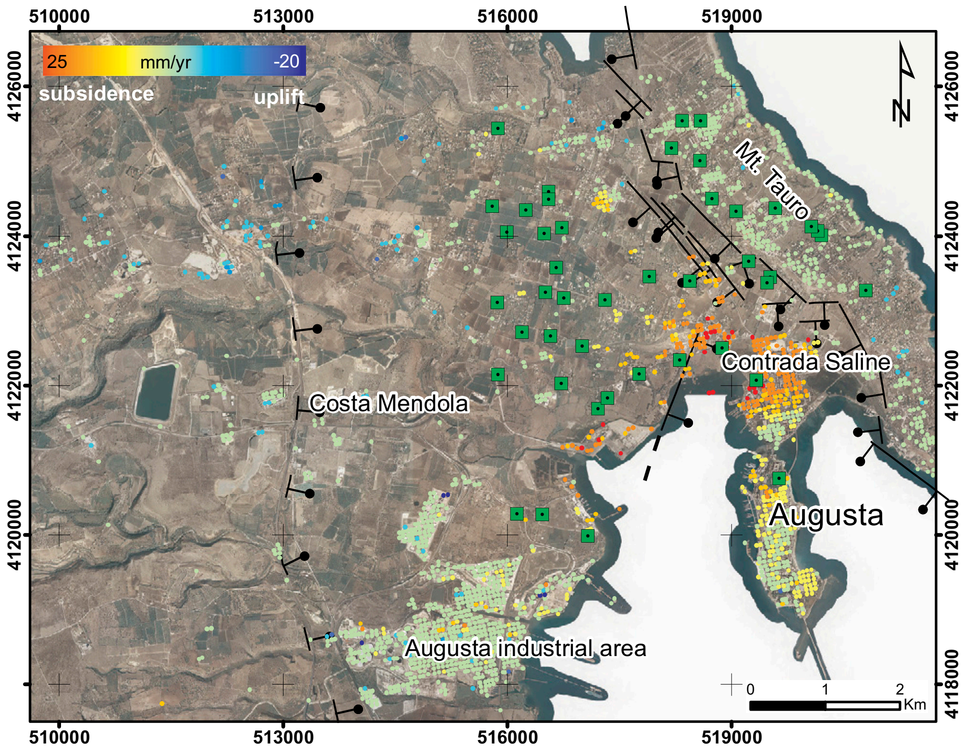

Figure 8. Differential interferometry synthetic aperture radar (DInSAR) mean displacement rates (mm/yr) retrieved in the 2004–2010 for ascending images. Wells (green boxes) and traces of the faults affecting the Quaternary marine terraces (as in Figs. 4 and 5, respectively) are also reported. Coordinates are referred to the UTM 33N grid zone.

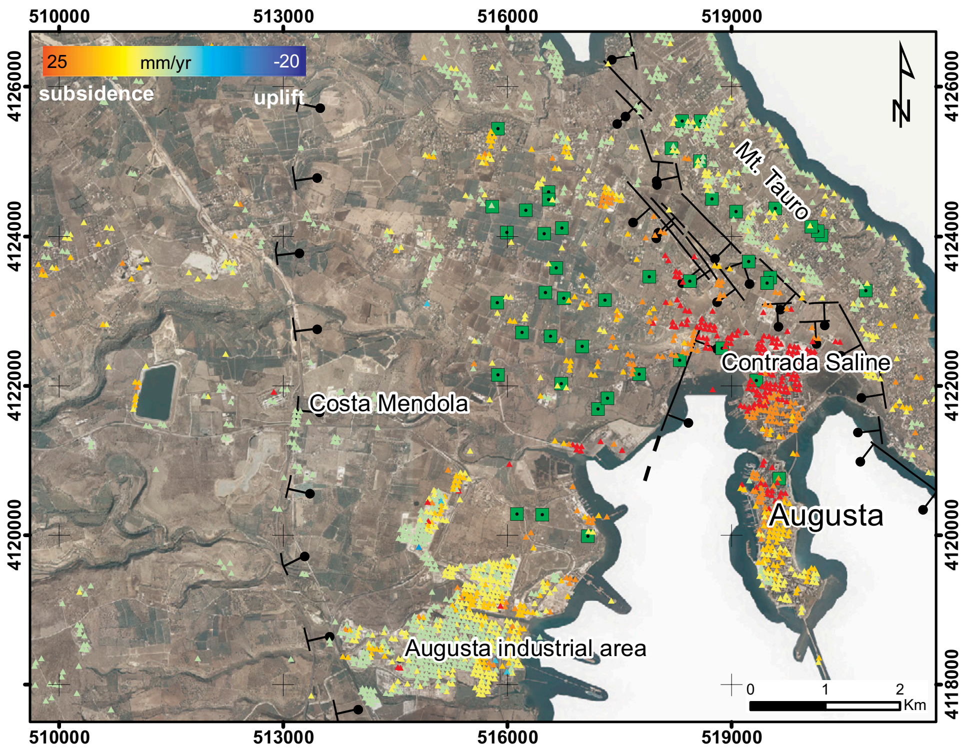

Figure 9. Differential interferometry synthetic aperture radar (DInSAR) mean displacement rates (mm/yr) retrieved in the 2003–2010 for descending images. Wells (green boxes) and traces of the faults affecting the Quaternary marine terraces (as in Figs. 4 and 5, respectively) are also reported. Coordinates are referred to the UTM 33N grid zone.

Lithosphere, published online on 6 July 2015 as doi:10.1130/L453.1

baselines as those of the ascending images were used. In this case, and for the reasons discussed already, two coherence threshold values were identified and set at 0.50 and 0.40, respectively. A measured displacement rate map was then constructed (Fig. 9).

The results of both processing analyses show the same sign (positive, i.e., displacements in the sensor-target direction), indicating that the predominant component of the displacement is the vertical over the horizontal one, as schematically shown in Figure 10.

As reported in Cascini et al. (2010), the combination of ascending and descending results allows the evaluation of vertical displacement rate (Fig. 11). The map in Figure 11 shows that the subsidence rate is highest to the north and west of the Augusta peninsula (in particular, around Contrada Saline site). It is worth pointing out that the spatial distribution of the highest displacement rates is independent from that of the wells, suggesting that the subsidence phenomenon is not correlated with water extraction. Figure 11 also shows that such subsidence rate tends to decrease with a radial pattern toward the west and south. On the other hand, a correlation of the deformation trend with anthropogenic factors may be envisaged in the Augusta industrial area. In this area, a slight subsidence increase is observed. Such increase is probably related to the presence of the main industrial installations (petrochemical) of the Augusta area, as suggested by Canova et al. (2012).

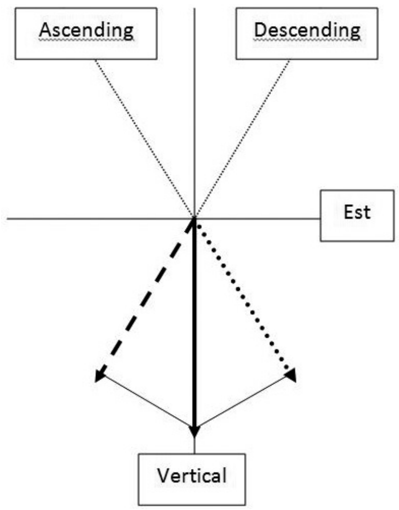

Figure 10. Example of entirely vertical displacement. The black arrow indicates the real displacement, while the dotted and dashed arrows indicate the ascending and descending components, respectively.

DISCUSSION

Data Interpretation

The onset of activity of the NW-SE–trending fault system controlling the Mendola horst may be inferred using the sedimentary record associated with related tectonic subsidence, as fault activity produced the accommodation space for syntectonic (i.e., synrift) deposits in this sector of the forebulge. Although a late Pliocene initiation of faulting, as originally suggested by Carbone (1985) and recently reproposed by I.S.P.R.A. (2011b) cannot be ruled out, it seems likely that the deposition of the Lower Pleistocene proximal calcarenites marks fault activity. These deposits may be interpreted as the coarser facies of the synrift succession, deposited close to the fault scarps. As demonstrated by Carbone (1985), these sediments pass laterally (toward the basin depocenters) and upward to Lower Pleistocene gray-bluish clays, which appear to represent the distal facies of the synrift succession, at least for their lower portion. In fact, the upper part of the gray-bluish clays, stratigraphically overlying the Lower Pleistocene proximal calcarenites and locally resting unconformably on top of the Miocene substratum, may be associated with a generalized postrift subsidence. It is worth noting that the model proposed by Carbone (1985) involves faulting during the Pliocene—a period characterized by a lack of sedimentation in the study area—and a cessation of fault activity by the early Pleistocene, when, according to Carbone, sedimentation would have been passively controlled by the preexisting paleobathymetry. Such a model appears to be inconsistent with the available stratigraphic data, as it implies a lack of a synrift sequence, which typically marks the activity of normal fault systems producing significant tectonic subsidence. Our interpretation is consistent with that proposed by Adam et al. (2000), who, for the NW-SE–trending fault system controlling the Mendola horst, referred to a tectonic collapse that led to the development of horsts and grabens at the beginning of the Pleistocene. It is worth noting that Carbone (1985), who suggested that the NW-SE–trending fault system was already "delineated" during the Pliocene, does not rule out its "reactivation" during the early Quaternary. On the other hand, cessation of differential vertical motions of the Mendola horst during the middle Pleistocene is constrained by coupled stratigraphic and geomorphological evidence. In fact, the faults bounding the horst are sealed by marine terraces and correlative deposits, which developed roughly parallel to the coast both across the Mendola horst and the adjacent grabens. In particular, the crosscutting relationships between the fault bounding the Costa Mendola ridge to the southwest and the marine terraces indicate that relative uplift of the Mendola horst at least predated the formation of the t4 marine terrace, which we tentatively correlate with the 330 ka MIS 9.3. The end of Mendola horst relative uplift is also inferred from the spatial distribution of the younger t3 marine terrace (that is carved in both the Mendola horst and adjacent graben blocks), and by the subsequent superimposition of the Torrente Molinello—and its left tributary—valley through the Costa Mendola ridge (Fig. 12). All this evidence indicates that

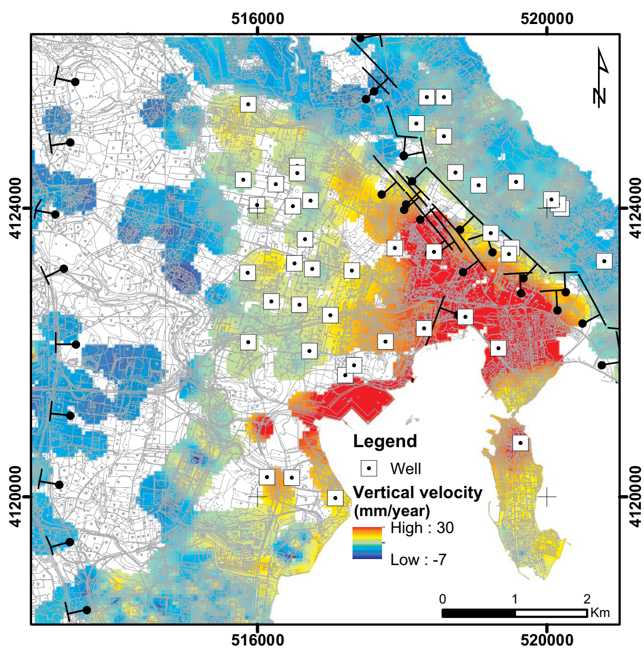

Figure 11. Vertical velocity component obtained by the combination of ascending and descending results. Wells and fault traces (as in Figs. 4 and 5, respectively) are also reported. Coordinates are referred to the UTM 33N grid zone.

Lithosphere, published online on 6 July 2015 as doi:10.1130/L453.1

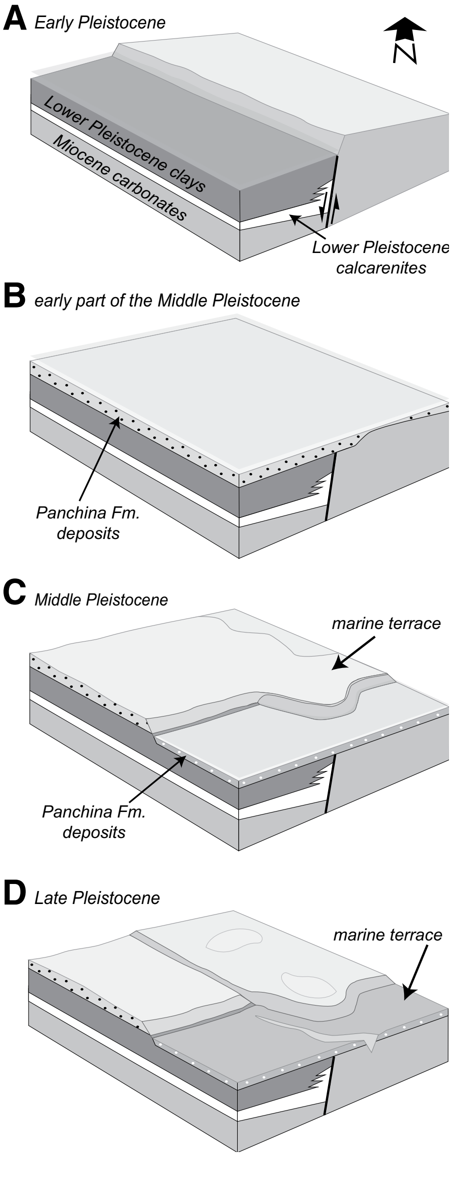

Figure 12. Cartoon showing the Quaternary evolution of the Costa Mendola area (transparent, light-gray layer indicates sea level). (A) During early Pleistocene, activity of the Costa Mendola fault controls deposition of the Lower Pleistocene calcarenites and clays. (B) In the early part of the middle Pleistocene, during sea-level rise and highstand, wave erosion (followed by deposition of the Panchina Formation calcarenites) causes retreat of the sea cliff formed along the now-inactive Costa Mendola fault, and formation of an abrasion platform on the footwall and hanging-wall blocks. (C) Later in the middle Pleistocene, the marine terrace created during the former stage is partly eroded in response to continuing uplift and sea-level fluctuations; the new sea-level rise and highstand are accompanied by uneven retreat—controlled by variable rock resistance to erosion—of the sea cliff, and calcarenite (Panchina Formation) deposition on the new wave-cut platform. (D) In the late Pleistocene, erosion and stream incision driven by further relative sea-level lowering affect the marine terraces formed in stages B and C; part of the veneer of shallow-marine sediments is eroded, causing partial exhumation of the paleo–sea cliff formed along the Costa Mendola fault during stage B.

normal fault activity is at least older than 400–300 ka. The DInSAR analysis clearly shows the lack of present-day vertical motions along the Costa Mendola fault.

On the other hand, the geomorphological evidence indicates that the NNW-SSE–trending Mount Tauro fault system has been active (or reactivated) in very recent times and has controlled the relative lowering of an area including the Augusta coastal plain. Significant constraints on the vertical motions in the town of Augusta and surrounding area have been obtained by the DInSAR analysis performed in this work. The analysis clearly highlights different vertical velocities affecting the footwall and hanging-wall blocks of the Mount Tauro fault system, with the latter block being subject to subsidence in the 2003–2010 time span. The pattern of vertical motions clearly points to a tectonic origin of the recorded vertical displacements, with the anthropogenic effects suggested by Canova et al. (2012) being minimal or even negligible, as is also inferred from hydrogeological information. This information indicates that the spatial distribution of high subsidence values is not correlated with that of the wells for water extraction (Fig. 11), and the lows in the groundwater surface of Figure 4. This lack of correlation suggests that the strong subsidence affecting the Augusta area in the 2003–2010 time span cannot be interpreted as the direct response to consolidation triggered by groundwater extraction/overexploitation, which dates to previous decades (a strong decline of the piezometric surface of the lower aquifer has been framed in the time span ranging from the 1960s to the 1980s; I.S.P.R.A., 2011b). In addition, since the Lower Pleistocene clays are overconsolidated, consolidation triggered by the decline of the piezometric surface would have affected only a limited part (i.e., the alluvial deposits and Lower Pleistocene calcarenites/sands; Fig. 3B) of the sedimentary succession overlying the Miocene carbonates in the Augusta Basin. All this evidence indicates that water extraction and related phenomena (essentially consolidation, taking into account that salt-wedge intrusion, although causing changes in the groundwater chemistry, is not responsible for subsidence) may only account for a small amount of the subsidence observed in the area to the southwest of the Mount Tauro fault system, although an anthropogenic contribution to subsidence of the Augusta industrial area (see section on "Interferometric Data Set and Results") may be envisaged. Furthermore, evidence for recent activity of NNW-SSE–trending faults in the Augusta area is consistent with information from offshore Augusta from Firetto Carlino et al. (2013) and Pirrotta et al. (2013), which points to vertical offset affecting seismic reflectors associated with Upper Pleistocene–Holocene deposits along NNW-SSE–trending faults (e.g., the Augusta offshore fault in Fig. 3B).

Tectonic Implications

Forebulge-related tectonic features discussed in this study provide further insights into the magnitude, modes, and timing of development of structures that are commonly incorporated in fold-and-thrust belts. These prethrusting structures may play an important role in subsequent deformation (e.g., Butler, 1989; Scisciani et al., 2001; Mazzoli et al., 2002; Tavarnelli and Peacock, 2002). Increasing evidence suggests that these features represent very important, widespread background structures in rocks later involved in fold-and-thrust belts (Calamita and Deiana, 1980; Scisciani et al., 2001; Lash and Engelder, 2007; Casini et al., 2011; Beaudoin et al., 2012; Quintà and Tavani, 2012; Tavani et al., 2012). Detailed structural surveys carried out by Billi et al. (2006) over the whole Hyblean Plateau documented coeval, multiple structural associations consisting of normal faults and joint systems. According to these authors, the development of two mutually orthogonal sets of major extensional structures occurred since Langhian time in response to bimodal stretching along both NW-SE and NE-SW directions. These results were consistently interpreted as evidence for the growth of a doubly plunging forebulge, controlled by the occurrence of foreland crustal heterogeneities. The latter would have also enhanced differential retreating processes of the foreland along the subduction zone and the subsequent formation of orogenic salients and recesses (Billi et al., 2006). Within this framework, strike-slip and extensional faulting along the Malta Escarpment and the Scicli Line (Grasso and Reuther, 1988; Grasso, 1993; Adam et al., 2000; Argnani and Bonazzi, 2005) is inferred to have accommodated part of the differential retreating kinematics of the Hyblean foreland monocline and part of the extensional strain induced by the doubly plunging flexure (Billi et al., 2006). The Costa Mendola normal fault, which was active for a time span in excess of 1 m.y. during the early to middle Pleistocene, appears to represent one of the most recent extensional structures associ-

Lithosphere, published online on 6 July 2015 as doi:10.1130/L453.1

ated with development of such a doubly plunging forebulge. In fact, earthquake fault plane solutions and borehole breakout data indicate that the present-day tectonic setting of the study area is dominated by NW-SE–oriented shortening and NE-SW extension, within the general framework of an active strike-slip regime (Ragg et al., 1999; Adam et al., 2000; Goes et al., 2004). This is also consistent with the principal strain-rate axes obtained from interpolation of the global positioning system (GPS)–derived velocity field over the study area (Devoti et al., 2011). Active shortening normal to the strike of the forebulge axis is clearly incompatible with the tectonic setting expected by bending around a roughly NE-trending horizontal axis as a result of flexure of the foreland plate. The deactivation of NW-SE–striking extensional structures such as the Costa Mendola fault discussed in this study further suggests that orthogonal bending around a NW-trending horizontal axis, characterizing the development of the doubly plunging forebulge (Billi et al., 2006), also ceased during the middle Pleistocene. All together, this evidence indicates that the rollback process controlling the tectonic evolution of the Maghrebian-Sicilian fold-and-thrust belt during Neogene to early Pleistocene times has come to a stop, similar to what has been documented for the Southern Apennine segment of the same orogen. There, a major geodynamic change occurred at the beginning of the middle Pleistocene (at ca. 0.7 Ma; e.g., Cinque et al., 1993), when complete slab detachment is inferred to have taken place, following a southeastward along-strike slab tear migration that initiated during the Pliocene, at ca. 4 Ma (Ascione et al., 2012). A similar process probably occurred in Sicily as a result of an eastward slab tear migration along strike of the Maghrebian-Sicilian belt (Neri et al., 2009), leading to the final complete slab breakoff in the Calabrian arc sector at ca. 0.7 Ma. Following this event, NW-oriented shortening associated with Africa-Eurasia plate convergence (Mazzoli and Helman, 1994) became dominant over both the Adriatic-Apulian and Hyblean forelands. Active deformation of the latter is consistent with that recorded across the whole North African continental margin south of Sicily, which is characterized by major E-W–trending, right-lateral, strike-slip fault zones along the Sicily Channel (e.g., Jongsma et al., 1985). This consistency provides further evidence for the Hyblean Plateau presently behaving as part of the larger Pelagian block, where lithospheric bending–related deformation has ceased in the forebulge sector. Indeed, significantly reduced or even negligible rates of southeastward motion of Calabria characterize the last 1 m.y. (Mattei et al., 2007; Johnston and Mazzoli, 2009), while GPS geodesy indicates that rapid southeastward motion of Calabria has stopped (D'Agostino and Selvaggi, 2004). Cessation of subduction (e.g., Westaway, 1993) is consistent with the observation that slow convergence across the Africa-Eurasia plate boundary (Mazzoli and Helman, 1994) is presently accommodated along a seismic belt dominated by thrust faulting offshore northern Sicily (e.g., Billi et al., 2007), rather than at the thrust front.

The earthquake focal mechanism pattern depicted in Figure 1 and the short-term vertical motions documented in this study in the Augusta–Mount Tauro area indicate that significant dip-slip extensional movements accompanied the dominant strike-slip tectonic regime that is active in SE Sicily. The middle Pleistocene to present uplift of SE Sicily, characterized by maximum values along the front of the Maghrebian-Sicilian belt and by a pattern of decreasing values to the south, is also consistent with the rebound effect following complete slab breakoff (Cinque et al., 1993; Ascione et al., 2012).

CONCLUSIONS

The integrated approach used in this study constrains the modes and duration of activity of Quaternary fault systems in a peculiar area of the African continental margin representing a foreland indentor during major plate convergence in the Mediterranean area. Modes of forebulge deformation, being strongly controlled by subduction dynamics, record a dramatic change in the slab configuration beneath the study area (Fig. 13).

Bimodal extension associated with bending of the foreland plate during the development of the doubly plunging Hyblean forebulge produced two mutually orthogonal normal fault systems, one parallel to the NE-trending main forebulge axis, and another parallel to the secondary NW-trending axis. Detailed analysis of the stratigraphic record allowed us to constrain the timing of activity—not older than ca. 1.8 Ma and not younger than ca. 0.3 Ma—of an extensional structure (the Costa Mendola fault) belonging to the NW-trending system. Therefore, this well-documented Pleistocene structure appears to have been active for not longer than ~1.5 m.y. during the latest stages of rollback associated with NW-directed subduction.

Subsequent late Quaternary to present deformation is dominated by regional uplift, progressively increasing toward the thrust front to the NW, and strike-slip faulting controlled by NW-oriented horizontal compression. Differential uplift within the Hyblean Plateau is accommodated by dip-slip components of motion along active NNW-trending structures such as the Monte Tauro fault. This fault probably forms part of the larger Malta Escarpment fault system, which is known to be active and characterized by large recent vertical offsets at the same latitude (Argnani and Bonazzi, 2005). The overall active tectonic setting—dominated by NW-oriented horizontal compression consistent with major plate convergence—and the regional uplift pattern characterizing the study area may be explained within the framework of intraplate shortening and foreland rebound following complete slab breakoff, a process that has been inferred to have occurred at ca. 0.7 Ma (Cinque et al., 1993; Ascione et al., 2012).

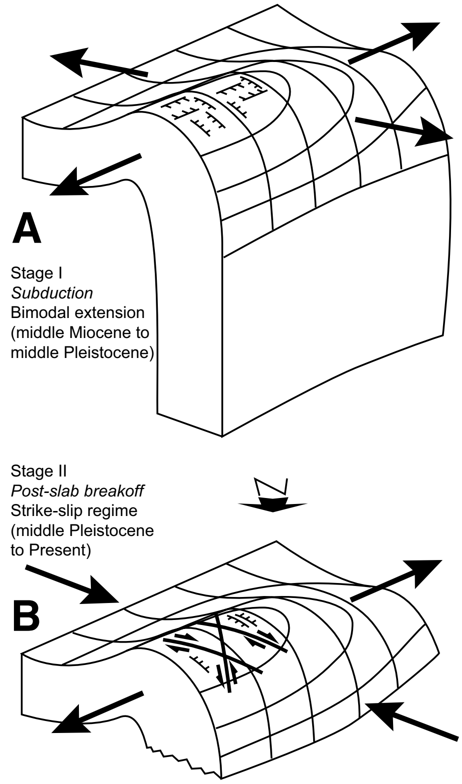

Figure 13. Summary of tectonic evolution of the Hyblean Plateau (diverging arrows indicate horizontal extension direction; converging arrows indicate horizontal shortening direction). (A) Bimodal extension associated with the development of a doubly plunging forebulge during subduction and slab rollback. (B) Strike-slip–dominated deformation postdating complete slab breakoff.

APPENDIX

SUBSOFT processor software, based on the coherent pixels technique (Mora et al., 2003; Blanco-Sánchez et al., 2008; Iglesias et al., 2014), implemented at the Remote Sensing Laboratory (RSLab) of the Universitat Politecnica de Catalunya (UPC), is able to extract the evolution of deformation from a stack of differential interferograms over wide areas during large time spans.

The SUBSOFT processor is composed of two utilities for interferometric processing, PRISAR and SUBSOFT. PRISAR consists of a set of routines implemented for the computation of the differential interferograms and the coherence maps; SUBSOFT is an application that uses PRISAR's output (differential interferograms and coherence maps) to extract the linear and nonlinear deformation evolution of the study area.

The interferometric process starts with PRISAR routine steps:

(1) The first step is selection of the best SLC image pairs among all the available images of the area under investigation. In order to carry out the selection, from all SLC images, the spatial baseline (distance between orbital positions), the temporal baseline (temporal distance between acquisitions), and the Doppler frequency (Df) are considered. The aim of this step is to identify the minimum number of interferograms in the stack that have the maximum quality overall.

(2) Starting from SLC images, coregistration between each image is carried out in order to evaluate the interferometric phase differences (interferogram). The coregistration consists in spatial registration and eventually resampling (SLC with different pixel size) in order to adjust for relative translational shift and rotational and scale differences.

(3) Precise satellite orbits and DTMs are used to create the differential interferograms and interferometric coherence maps.

From these outcomes, the SUBSOFT routine is implemented:

(4) Since not all pixels are characterized by stable phase, a pixel selection is carried out. The SUBSOFT processor is implemented with different criteria of selection: coherence stability (Berardino et al., 2002), amplitude dispersion (Ferretti et al., 2000), and temporal sublook coherence (Iglesias et al., 2014).

(5) The last step consists of phase analysis to calculate linear and nonlinear components of deformation. Through the linear model, a measured displacement rate map is obtained, while the nonlinear model allows time series of deformations to be obtained.

ACKNOWLEDGMENTS

We wish to thank Andrea Billi, an anonymous reviewer, and Editor Arlo Weil for their thoughtful and constructive reviews, which substantially helped us to improve the manuscript.

REFERENCES CITED

Accordi, B., 1962, Some data on the Pleistocene stratigraphy and related pigmy mammalian faunas of eastern Sicily: Quaternaria, v. 6, p. 415–430.

Accordi, B., 1963, Rapporti fra il "Milazziano" della costa iblea (Sicilia sudorientale) e la comparsa di *Elephas mnaidriensis*: Geologica Romana, v. 2, p. 295–304.

Adam, J., Reuther, C.D., Grasso, M., and Torelli, L., 2000, Active fault kinematics and crustal stresses along the Ionian margin of southeastern Sicily: Tectonophysics, v. 326, no. 3–4, p. 217–239, doi:10.1016/S0040-1951(00)00141-4.

Agocs, W.B., 1959, Profondità e struttura dell'orizzonte igneo fra Catania e Tunisi dedotte da un profilo aeromagnetico: Bollettino del Servizio Geologico Italiano, v. 80, p. 51–61.

Amato, A., Azzara, R., Basili, A., Chiarabba, C., Cocco, M., Di Bona, M., and Selvaggi, G., 1995, Main shock and aftershocks of the December 13, 1990, Eastern Sicily earthquake: Annals of Geophysics, v. 38, no. 2, p. 255–266.

Antonelli, M., Franciosi, R., Pezzi, G., Querci, A., Ronco, G.P., and Vezzani, F., 1988, Paleogeographic evolution and structural setting of the northern side of the Sicily Channel: Memorie della Società Geologica Italiana, v. 41, p. 141–157.

Antonioli, F., Kershaw, S., Rust, D., and Verrubbi, V., 2003, Holocene sea-level change in Sicily and its implications for tectonic models: New data from the Taormina area, northeast Sicily: Marine Geology, v. 196, no. 1–2, p. 53–71, doi:10.1016/S0025-3227(03)00029-X.

Antonioli, F., Kershaw, S., Renda, P., Rust, D., Belluomini, G., Cerasoli, M., Radtke, U., and Silenzi, S., 2006, Elevation of the Last Interglacial highstand in Sicily (Italy): A benchmark of coastal tectonics: Quaternary International, v. 145–146, p. 3–18, doi:10.1016/j.quaint.2005.07.002.

Antonioli, F., Ferranti, L., Fontana, A., Amorosi, A.M., Bondesan, A., Braitenberg, C., Dutton, A., Fontolan, G., Furlani, S., Lambeck, K., Mastronuzzi, G., Monaco, C., Spada, G., and Stocchi, P., 2009, Holocene relative sea-level changes and vertical movements along the Italian and Istrian coastlines: Quaternary International, v. 206, p. 102–133, doi:10.1016/j.quaint.2008.11.008.

Argnani, A., and Bonazzi, C., 2005, Malta Escarpment fault zone offshore eastern Sicily: Pliocene–Quaternary tectonic evolution based on new multichannel data: Tectonics, v. 24, p. TC4009, doi:10.1029/2004TC001656.

Arnaud, A., Adam, N., Hanssen, R., Inglada, J., Duro, J., Closa, J., and Eineder, M., 2003, ASAR ERS interferometric phase continuity, *in* Proceedings of the IEEE (Institute of Electrical and Electronic Engineers) International Geoscience and Remote Sensing Symposium (IGARSS '03), 21–25 July 2003, Toulouse (France), v. 2, p. 1133–1135.

Ascione, A., Ciarcia, S., Di Donato, V., Mazzoli, S., and Vitale, S., 2012, The Pliocene–Quaternary wedge-top basins of southern Italy: An expression of propagating lateral slab tear beneath the Apennines: Basin Research, v. 24, p. 456–474, doi:10.1111/j.1365-2117.2011.00534.x.

Aureli, A., Adorni, G., Chiavetta, A.F., Fazio, F., Fazzina, S., and Messineo, G., 1987a, Carta idrogeologica di una regione ove sono presenti acquiferi sovrasfruttati: Memorie della Società Geologica Italiana, v. 37, p. 27–34.

Aureli, A., Adorni, G., Chiavetta, A.F., and Fazio, F., 1987b, Condizioni di vulnerabilità di acquiferi in zona a forte insediamento industriale di tipo petrolchimico: Memorie della Società Geologica Italiana, v. 37, p. 35–52.

Azienda Generale Italiana Petroli (AGIP), 1978, Carta Gravimetrica della Sicilia, Anomalie di Bouguer: Bollettino del Servizio Geologico Italiano 99, scale 1:500,000.

Azienda Generale Italiana Petroli (AGIP), 1982, Carta Magnetica, Anomalie del Campo Magnetico Residuo: S. Donato Milanese, Azienda Generale Italiana Petroli, scale 1:500,000.

Azzaro, R., and Barbano, M.S., 2000, Analysis of the seismicity of southeastern Sicily: A proposed tectonic interpretation: Annali di Geofisica, v. 43, no. 1, p. 171–188.

Azzaro, R., Barbano, M.S., Rigano, R., and Antichi, B., 2000, Contributo alla revisione delle zone sismogenetiche della Sicilia, *in* Galadini, F., Meletti, C., and Rebez, A., eds., Le Ricerche del GNDT nel Campo della Pericolosità Sismica (1996–99): Roma, CNR-Gruppo Nazionale per la Difesa Terremoti, p. 31–38.

Barrier, E., 1992, Tectonic analysis of a flexed foreland: The Ragusa Platform: Tectonophysics, v. 206, p. 91–111, doi:10.1016/0040-1951(92)90370-L.

Beaudoin, N., Leprêtre, R., Bellahsen, N., Lacombe, O., Amrouch, K., Callot, J.P., Emmanuel, L., and Daniel, J.M., 2012, Structural and microstructural evolution of the Rattlesnake Mountain anticline (Wyoming, USA): New insights into the Sevier and Laramide orogenic stress build up in the Bighorn Basin: Tectonophysics, v. 576–577, p. 20–45, doi:10.1016/j.tecto.2012.03.036.

Ben-Avraham, Z., Lyakhovsky, V., and Grasso, M., 1995, Simulation of collision zone segmentation in the central Mediterranean: Tectonophysics, v. 243, no. 1–2, p. 57–68, doi:10.1016/0040-1951(94)00191-B.

Berardino, P., Fornaro, G., Lanari, R., and Sansosti, E., 2002, A new algorithm for surface deformation monitoring based on small baseline differential SAR interferograms: IEEE Transactions on Geoscience and Remote Sensing, v. 40, no. 11, p. 2375–2383, doi:10.1109/TGRS.2002.803792.

Bianca, M., Monaco, C., Tortorici, L., and Cernobori, L., 1999, Quaternary normal faulting in southeastern Sicily (Italy): A seismic source for the 1693 large earthquake: Geophysical Journal International, v. 139, no. 2, p. 370–394, doi:10.1046/j.1365-246x.1999.00942.x.

Bianchi, F., Carbone, S., Grasso, M., Invernizzi, G., Lentini, F., Longaretti, G., Merlini, S., and Mostardini, F., 1987, Sicilia orientale: Profilo geologico Nebrodi-Iblei: Memorie della Società Geologica Italiana, v. 38, p. 429–458.

Billi, A., 2005, Grain size distribution and thickness of breccia and gouge zones from thin (<1m) strike-slip fault cores in limestone: Journal of Structural Geology, v. 27, no. 10, p. 1823–1837, doi:10.1016/j.jsg.2005.05.013.

Billi, A., and Salvini, F., 2003, Development of systematic joints in response to flexure-related fibre stress in flexed foreland plates: The Apulian forebulge case history, Italy: Journal of Geodynamics, v. 36, no. 4, p. 523–536, doi:10.1016/S0264-3707(03)00086-3.

Billi, A., Porreca, M., Faccenna, C., and Mattei, M., 2006, Magnetic and structural constraints for the noncylindrical evolution of a continental forebulge (Hyblea, Italy): Tectonics, v. 25, p. TC3011, doi:10.1029/2005TC001800.

Billi, A., Presti, D., Faccenna, C., Neri, G., and Orecchio, B., 2007, Seismotectonics of the Nubia plate compressive margin in the south-Tyrrhenian region, Italy: Clues for subduction inception: Journal of Geophysical Research, v. 112, p. B08302, doi:10.1029/2006JB004837.

Billi, A., Presti, D., Orecchio, B., Faccenna, C., and Neri, G., 2010, Incipient extension along the active convergent margin of Nubia in Sicily, Italy: Cefalù-Etna seismic zone: Tectonics, v. 29, p. TC4026, doi:10.1029/2009TC002559.

Blanco-Sánchez, P., Mallorquí, J.J., Duque, S., and Monells, D., 2008, The coherent pixels technique (CPT): An advanced DInSAR technique for non-linear deformation monitoring: Pure and Applied Geophysics, v. 165, p. 1167–1193, doi:10.1007/s00024-008-0352-6.

Bolis, G., Carruba, S., Casnedi, R., Perotti, C.R., Ravaglia, A., and Tornaghi, M., 2003, Compressional tectonics overprinting extensional structures in the Abruzzo Periadriatic foredeep (central Italy) during Pliocene times: Bollettino della Società Geologica Italiana, v. 122, no. 2, p. 251–266.

Bordonaro, S., Di Grande, A., and Raimondo, W., 1984, Lineamenti geomorfostratigrafici pleistocenici tra Melilli, Augusta e Lentini (Siracusa): Bollettino Accademia Gioenia di Scienze Naturali Catania, v. 323, no. 17, p. 65–88.

Bordoni, P., and Valensise, G., 1998, Deformation of the 125 ka marine terrace in Italy: Tectonic implications, *in* Stewart, I.S., Vita-Finzi, C., eds., Coastal Tectonics: Geological Society of London Special Publication 146, p. 71–110, doi:10.1144/GSL.SP.1999.146.01.05.

Bradley, D.C., and Kidd, W.S.F., 1991, Flexural extension of the upper continental crust in collisional foredeeps: Geological Society of America Bulletin, v. 103, no. 11, p. 1416–1438, doi:10.1130/0016-7606(1991)103<1416:FEOTUC>2.3.CO;2.

Burollet, P.F., Mugniot, G.M., and Sweeney, P., 1978, Geology of the Pelagian block: The margin and basin of southern Tunisia and Tripolitania, *in* Nairn, A., Kanes, W., and Stelhi, F.G., eds., The Ocean Basin and Margin: New York, Plenum, p. 331–419.

Butler, R.W.H., 1989, The influence of pre-existing basin structure on thrust system evolution in the western Alps, *in* Cooper, M.A., and Williams, G.D., eds., Inversion Tectonics: Geological Society of London Special Publication 44, p. 105–122, doi:10.1144/GSL.SP.1989.044.01.07.

Butler, R.W.H., Grasso, M., and La Manna, F., 1992, Origin and deformation of the Neogene–Recent Maghrebian foredeep at the Gela Nappe, SE Sicily: Journal of the Geological Society of London, v. 149, p. 547–556, doi:10.1144/gsjgs.149.4.0547.

Butler, R.W.H., Lickorish, W.H., Grasso, M., Pedley, H.M., and Ramberti, L., 1995, Tectonic and sequence stratigraphy in Messinian basins, Sicily: Constraints on the initiation and termination of the Messinian salinity crisis: Geological Society of America Bulletin, v. 107, p. 425–439, doi:10.1130/0016-7606(1995)107<0425:TASSIM>2.3.CO;2.

Caire, A., 1970, Sicily in its Mediterranean setting, *in* Alvarez, W., and Gohrbandt, K.H.A., eds., Geology and History of Sicily: Tripoli, Petroleum Exploration Society of Lybia, p. 145–170.

Calamita, F., and Deiana, G., 1980, Evidenze di una fase tettonica distensiva del Messiniano basale nel bacino di Camerino (Appennino umbro-marchigiano): Studi Geologici Camerti, v. 7, p. 7–11.

Canova, F., Tolomei, C., Salvi, S., Toscani, G., and Seno, S., 2012, Land subsidence along the Ionian coast of SE Sicily (Italy), detection and analysis via small baseline subset (SBAS) multitemporal differential SAR interferometry: Earth Surface Processes and Landforms, v. 37, no. 3, p. 273–286, doi:10.1002/esp.2238.

Carbone, S., 1985, I depositi Pleistocenici del settore orientale ibleo tra Agnone e Melilli (Sicilia SE): Relazione tra facies e lineamenti strutturali: Bollettino della Società Geologica Italiana, v. 104, p. 405–420.

Carbone, S., Di Geronimo, I., Grasso, M., Iozzia, S., and Lentini, F., 1982a, I terrazzi marini quaternari dell'area iblea (Sicilia Sud-Orientale), in Contributi conclusivi per la realizzazione della Carta Neotettonica d'Italia: CNR, Progetto Finalizzato Geodinamica Pubblicazione 506, p. 1–35.

Carbone, S., Cosentino, M., Grasso, M., Lentini, F., Lombardo, G., and Patanè, G., 1982b, Elementi per una prima valutazione dei caratteri sismotettonici dell'Avampaese Ibleo (Sicilia Sud-Orientale): Memorie della Società Geologica Italiana, v. 24, p. 507–520.

Carbone, S., Grasso, M., and Lentini, F., 1982c, Considerazioni sull'evoluzione geodinamica della Sicilia sud-orientale dal Cretaceo al Quaternario: Memorie della Società Geologica Italiana, v. 24, p. 362–386.

Carbone, S., Grasso, M., and Lentini, F., 1986, Carta Geologica del Settore Nordorientale Ibleo (Sicilia S-E): Firenze, S.EL. CA (Società Elaborazioni Cartografiche)., scale 1:50,000.

Carbone, S., Grasso, M., and Lentini, F., 1987, Lineamenti geologici del Plateau Ibleo (Sicilia S-E): Presentazione delle carte geologiche della Sicilia sud-orientale: Memorie della Società Geologica Italiana, v. 38, p. 127–135.

Cascini, L., Fornaro, G., and Peduto, D., 2010, Advanced low- and full-resolution DInSAR map generation for slow-moving landslide analysis at different scales: Engineering Geology, v. 112, p. 29–42, doi:10.1016/j.enggeo.2010.01.003.

Casini, G., Gillespie, P.A., Vergés, J., Romaire, I., Fernández, N., Casciello, E., and Hunt, D.W., 2011, Sub-seismic fractures in foreland fold and thrust belts: Insight from the Lurestan Province, Zagros Mountains, Iran: Petroleum Geoscience, v. 17, no. 3, p. 263–282, doi:10.1144/1354-079310-043.

Casnedi, R., 1988, La Fossa bradanica: origine, sedimentazione e migrazione: Memorie della Società Geologica Italiana, v. 41, p. 439–448.

Catalano, S., and De Guidi, G., 2003, Late Quaternary uplift of northeastern Sicily: Relation with the active normal faulting deformation: Journal of Geodynamics, v. 36, no. 4, p. 445–467, doi:10.1016/S0264-3707(02)00035-2.

Catalano, S., De Guidi, G., Romagnoli, G., Torrisi, S., Tortorici, G., and Tortorici, L., 2008, The migration of plate boundaries in SE Sicily: Influence on the large-scale kinematic model of the African promontory in southern Italy: Tectonophysics, v. 449, no. 1–4, p. 41–62, doi:10.1016/j.tecto.2007.12.003.

Catalano, S., Romagnoli, G., and Tortorici, G., 2010, Kinematics and dynamics of the late Quaternary rift-flank deformation in the Hyblean Plateau (SE Sicily): Tectonophysics, v. 486, p. 1–14, doi:10.1016/j.tecto.2010.01.013.

Cinque, A., Patacca, E., Scandone, P., and Tozzi, M., 1993, Quaternary kinematic evolution of the Southern Apennines. Relationships between surface geological features and deep lithospheric structures: Annals of Geophysics, v. 36, no. 2, p. 249–260.

Continisio, R., Ferrucci, F., Gaudiosi, G., Lo Bascio, D., and Ventura, G., 1997, Malta Escarpment and Mt. Etna: Early stages of an asymmetric rifting process? Evidences from geophysical and geological data: Acta Vulcanologica, v. 9, no. 1/2, p. 45–53.

Cosentino, D., and Gliozzi, E., 1988, Considerazioni sulle velocità di sollevamento di depositi eutirreniani dell'Italia meridionale e della Sicilia: Memorie della Società Geologica Italiana, v. 41, p. 653–665.

Costantini, M., Falco, S., Malvarosa, F., and Minati, F., 2008, A new method for identification and analysis of persistent scatterers in series of SAR images, *in* Proceedings of the IEEE (Institute of Electrical and Electronic Engineers)Proceedings of the International Geoscience and Remote Sensing Symposium (IGARSS '08), Boston, Massachusetts, 7–11 July 2008, p. 449–452.

D'Agostino, N., and Selvaggi, G., 2004, Crustal motion along the Eurasia-Nubia plate boundary in the Calabrian arc and Sicily and active extension in the Messina Straits from GPS measurements: Journal of Geophysical Research, v. 109, p. B11402, doi:10.1029/2004JB002998.

Dall'Antonia, B., Di Stefano, A., and Foresi, L.M., 2001, Integrated micropalaeontological study (ostracods and calcareous plankton) of the Langhian western Hyblean successions (Sicily, Italy): Palaeogeography, Palaeoclimatology, Palaeoecology, v. 176, no. 1-4, p. 59–80, doi:10.1016/S0031-0182(01)00326-1.

Destro, N., 1995, Release fault: A variety of cross fault in linked extensional fault systems, in the Sergipe-Alagoas Basin, NE Brazil: Journal of Structural Geology, v. 17, no. 5, p. 615–629, doi:10.1016/0191-8141(94)00088-H.

Devoti, R., Esposito, A., Pietrantonio, G., Pisani, A.R., and Riguzzi, F., 2011, Evidence of large scale deformation patterns from GPS data in the Italian subduction boundary: Earth and Planetary Science Letters, v. 311, no. 3–4, p. 230–241, doi:10.1016/j.epsl.2011.09.034.

Di Geronimo, I., Ghisetti, F., Lentini F. and Vezzani, L., 1978, Lineamenti neotettonici della Sicilia orientale: Memorie Società Geologica Italiana, v. 19, p. 543–549.

Di Grande, A., 1972, Geologia dell'area a nord di Augusta-Francofonte (Sicilia SE): Atti Accademia Gioenia Catania, ser. 7, v. 4, 32 p.

Di Grande, A., and Neri, M., 1988, Tirreniano a *Strombus b.* a M. Tauro (Augusta, Siracusa): Rendiconti della Società Geologica Italiana, v. 11, p. 57–58.

Di Grande, A., and Raimondo, W., 1982, Linee di costa plio-pleistoceniche e schema litostratigrafico del Quaternario siracusano: Geologica Romana, v. 21, p. 279–309.

Di Grande, A., and Scamarda, G., 1973, Segnalazione di livelli a *Strombus bubonius* LAMARK nei dintorni di Augusta (Siracusa): Bollettino Accademia Gioenia di Scienze Naturali Catania, ser. 4, v. 11, no. 9–10, p. 157–172.

Di Stefano, A., and Branca, S., 2002, Long-term uplift rate of the Etna volcano basement (southern Italy) based on biochronological data from Pleistocene sediments: Terra Nova, v. 14, no. 1, p. 61–68, doi:10.1046/j.1365-3121.2002.00389.x.

Doglioni, C., 1995, Geological remarks on the relationships between extension and convergent geodynamic settings: Tectonophysics, v. 252, p. 253–267, doi:10.1016/0040-1951(95)00087-9.

Duro, J., Closa, J., Biescas, E., Crosetto, M., and Arnaud, A., 2005, High resolution differential interferometry using time series of ERS and ENVISAT SAR data, *in* Proceedings of the 6th Geomatic Week Conference, February 2005: Barcelona, Spain, CD-ROM (unpaginated).

Ferranti, L., Antonioli, F., Mauz, B., Amorosi, A., Dai Pra, G., Mastronuzzi, G., Monaco, C., Orrù, P., Pappalardo, M., Radtke, U., Renda, P., Romano, P., Sansò, P., and Verrubbi, V., 2006, Markers of the last interglacial sea level high stand along the coast of Italy: Tectonic implications: Quaternary International, v. 145–146, p. 30–54, doi:10.1016/j.quaint.2005.07.009.

Ferretti, A., Prati, C., and Rocca, F., 2000, Nonlinear subsidence rate estimation using permanent scatterers in differential SAR interferometry: IEEE Transactions on Geoscience and Remote Sensing, v. 38, no. 5, p. 2202–2212, doi:10.1109/36.868878.

Ferretti, A., Tamburini, A., Novali, F., Fumagalli, A., Falorni, G., and Rucci, A., 2011, Impact of high resolution radar imagery on reservoir monitoring: Energy Procedia, v. 4, p. 3465–3471, doi:10.1016/j.egypro.2011.02.272.

Firetto Carlino, M., Di Stefano, A., and Budillon, F., 2013, Seismic facies and seabed morphology in a tectonically controlled continental shelf: The Augusta Bay (offshore eastern Sicily, Ionian Sea): Marine Geology, v. 335, p. 35–51, doi:10.1016/j.margeo.2012.10.009.

Geiser, P., and Engelder, T., 1983, The distribution of layer parallel shortening fabrics in the Appalachian foreland of New York and Pennsylvania: Evidence for two non-coaxial phases of the Alleghanian orogeny, *in* Hatcher, R.D., Jr., Williams, H., and Zietz, I., eds., Contributions to the Tectonics and Geophysics of Mountain Chains: Geological Society of America Memoir 158, p. 161–175.

Gignoux, M., 1913, Les Formations Marines du Pliocènes et Quaternaires de l'Italie du Sud et de la Sicile: Annales Université Lyon 36, 693 p.

Goes, S., Giardini, D., Jenny, S., Hollenstein, C., Kahle, H.G., and Geiger, A., 2004, A recent tectonic reorganization in the south-central Mediterranean: Earth and Planetary Science Letters, v. 226, p. 335–345, doi:10.1016/j.epsl.2004.07.038.

Grasso, M., 1993, Pleistocene structures along the Ionian side of the Hyblean Plateau (SE Sicily): Implications for the tectonic evolution of the Malta Escarpment, *in* Max, M.D., and Colantoni, P., eds., Geological Development of the Sicilian-Tunisian Platform: UNESCO Reports in Marine Science 58, p. 49–54.

Grasso, M., and Lentini, F., 1982, Sedimentary and tectonic evolution of the eastern Hyblean Plateau (southeast Sicily) during Late Cretaceous to Quaternary time: Palaeogeography, Palaeoclimatology, Palaeoecology, v. 39, p. 261–280, doi:10.1016/0031-0182(82)90025-6.

Grasso, M., and Pedley, H.M., 1990, Neogene and Quaternary sedimentation patterns in the northwestern Hyblean Plateau (SE Sicily): The effects of a collisional process on a foreland margin: Rivista Italiana di Paleontologia e Stratigrafia, v. 96, no. 2–3, p. 219–240.

Grasso, M., and Reuther, C.D., 1988, The western margin of the Hyblean Plateau: A neotectonic transform system on the SE Sicilian foreland: Annales Tectonicae, v. 2, p. 107–120.

Grasso, M., Lentini, F., Nairn, A.E.M., and Vigliotti, L., 1983, A geological and paleomagnetic study of the Hyblean volcanic rocks, Sicily: Tectonophysics, v. 98, p. 271–295, doi:10.1016/0040-1951(83)90298-6.

Grasso, M., De Dominicis, A., and Mazzoldi, G., 1990, Structures and tectonic setting of the western margin of the Hyblean-Malta Shelf, central Mediterranean: Annales Tectonicae, v. 4, p. 140–154.

Grasso, M., Philps, B., Reuther, C.D., Garofalo, P., Stamilla, R., Anfuso, G., Donzella, G., and Cultrone, G., 2000, Pliocene–Pleistocene tectonics on western margin of the Hyblean Plateau and the Vittoria Plain (SE Sicily): Memorie della Società Geologica Italiana, v. 55, p. 35–44.

Hanssen, R., 2001, Radar Interferometry: Dordrecht, The Netherlands, Kluwer Academic Publishers, 308 p.

Hirn, A., Nicolich, R., Gallart, J., Laigle, M., and Cernobori, L., and ETNASEIS Scientific Group, 1997, Roots of Etna volcano in faults of great earthquakes: Earth and Planetary Science Letters, v. 148, no. 1–2, p. 171–191, doi:10.1016/S0012-821X(97)00023-X.

Hooper, A., 2008, A multi-temporal InSAR method incorporating both persistent scatterer and small baseline approaches: Geophysical Research Letters, v. 35, p. L16302, doi:10.1029/2008GL034654.

Hooper, A., Zebker, H., Segall, P., and Kampes, B., 2004, A new method for measuring deformation on volcanoes and other natural terrains using InSAR persistent scatterers: Geophysical Research Letters, v. 31, p. L23611, doi:10.1029/2004GL021737.

Iglesias, R., Mallorqui, J.J., and Lopez-Dekker, P., 2014, DInSAR pixel selection based on sublook spectral correlation along time: IEEE Transactions on Geoscience and Remote Sensing, v. 52, p. 3788–3799, doi:10.1109/TGRS.2013.2276023.

Istituto Superiore di Protezione e Ricerca Ambientale (I.S.P.R.A.), 2011a, Carta Geologica d'Italia alla, Foglio 641 "Augusta": Roma, I.S.P.R.A., Servizio Geologico d'Italia, scale 1:50,000, http://www.isprambiente.gov.it/Media/carg/641_AUGUSTA/Foglio.html.

Istituto Superiore di Protezione e Ricerca Ambientale (I.S.P.R.A.), 2011b, Note illustrative della Carta Geologica d'Italia alla scale 1:50,000, Foglio 641 "Augusta": Roma, I.S.P.R.A., Servizio Geologico d'Italia, p. 247, http://www.isprambiente.gov.it/Media/carg/note_illustrative/641_Augusta.pdf.

Johnston, S.T., and Mazzoli, S., 2009, The Calabrian orocline: Buckling of a previously more linear orogen, *in* Murphy, J.B., Keppie J.D., and Hynes A.J., eds., Ancient Orogens and Modern Analogues: Geological Society of London Special Publication 327, p. 113–125.

Jongsma, D., van Hinte, J.E., and Woodside, J.M., 1985, Geologic structure and neotectonics of the North African continental margin south of Sicily: Marine and Petroleum Geology, v. 2, no. 2, p. 156–179, doi:10.1016/0264-8172(85)90005-4.

Krzywiec, P., 2001, Contrasting tectonic and sedimentary history of the central and eastern parts of the Polish Carpathian foredeep basin—Results of seismic data interpretation: Marine and Petroleum Geology, v. 18, no. 1, p. 13–38, doi:10.1016/S0264-8172(00)00037-4.

Lambeck, K., Antonioli, F., Anzidei, M., Ferranti, L., Leoni, G., Scicchitano, G., and Silenzi, S., 2011, Sea level change along the Italian coast during the Holocene and projections for the future: Quaternary International, v. 232, no. 1–2, p. 250–257, doi:10.1016/j.quaint.2010.04.026.

Lanari, R., Mora, O., Manunta, M., Mallorqui, J.J., Berardino, P., and Sansosti, E., 2004, A small baseline approach for investigating deformations on full resolution differential SAR interferograms: IEEE Transactions on Geoscience and Remote Sensing, v. 42, p. 1377–1386, doi:10.1109/TGRS.2004.828196.

Langhi, L., Ciftci, N.B., and Borel, G.D., 2011, Impact of lithospheric flexure on the evolution of shallow faults in the Timor foreland system: Marine Geology, v. 284, no. 1–4, p. 40–54, doi:10.1016/j.margeo.2011.03.007.

Lash, G.G., and Engelder, T., 2007, Jointing within the outer arc of a forebulge at the onset of the Alleghanian orogeny: Journal of Structural Geology, v. 29, no. 5, p. 774–786, doi:10.1016/j.jsg.2006.12.002.

Lentini, F., Di Geronimo, I., Grasso, M., Carbone, S., Sciuto, E., Scamarda, G., Cugno, G., Iozzia, S., Bommarito, S., and La Rosa, N., 1984, Carta Geologica della Sicilia

Sud-Orientale: Florence, S.EL.CA. (Società Elaborazioni Cartografiche) ed., scale 1:100,000.

Lentini, F., 1983, The geology of the Mt. Etna basement: Memorie della Società Geologica Italiana, v. 23, p. 7–25.

Lisiecki, L.E., and Raymo, M.E., 2005, A Pliocene-Pleistocene stack of 57 globally distributed benthic $\delta^{18}O$ records: Paleoceanography, v. 20, p. PA1003, doi:10.1029/2004PA001071.

Lorenzo, J.M., O'Brien, G.W., Stewart, J., and Tandon, K., 1998, Inelastic yielding and forebulge shape across a modern foreland basin: North West Shelf of Australia, Timor Sea: Geophysical Research Letters, v. 25, no. 9, p. 1455–1458, doi:10.1029/98GL01012.

Maillard, A., Mauffret, A., Watts, A.B., Torné, M., Pascal, G., Buhl, P., and Pinet, B., 1992, Tertiary sedimentary history and structure of the Valencia trough (western Mediterranean): Tectonophysics, v. 203, no. 1–4, p. 57–75, doi:10.1016/0040-1951(92)90215-R.

Matenco, L., and Bertotti, G., 2000, Tertiary tectonic evolution of the external East Carpathians (Romania): Tectonophysics, v. 316, no. 3–4, p. 255–286, doi:10.1016/S0040-1951(99)00261-9.

Mattei, M., Cifelli, F., and D'Agostino, N., 2007, The evolution of the Calabrian arc: Evidence from palaeomagnetic and GPS observations: Earth and Planetary Science Letters, v. 263, p. 259–274, doi:10.1016/j.epsl.2007.08.034.

Mazzoli, S., and Helman, M., 1994, Neogene patterns of relative plate motion for Africa–Europe: Some implications for recent central Mediterranean tectonics: Geologische Rundschau, v. 83, p. 464–468.

Mazzoli, S., Barkham, S., Cello, G., Gambini, R., Mattioni, L., Shiner, P., and Tondi, E., 2001, Reconstruction of continental margin architecture deformed by the contraction of the Lagonegro Basin, Southern Apennines, Italy: Journal of the Geological Society of London, v. 158, p. 309–319, doi:10.1144/jgs.158.2.309.

Mazzoli, S., Deiana, G., Galdenzi, S., and Cello, G., 2002, Miocene fault-controlled sedimentation and thrust propagation in the previously faulted external zones of the Umbria–Marche Apennines, Italy, *in* Bertotti, G., Schulmann, K., and Cloetingh, S.A.P.L., eds., Continental collision and the tectono-sedimentary evolution of forelands: European Geophysical Union Stephan Mueller Special Publication 1 Series, v. 1, p. 195–209, doi:10.5194/smsps-1-195-2002.

Mazzoli, S., D'Errico, M., Aldega, L., Corrado, S., Invernizzi, C., Shiner, P., and Zattin, M., 2008, Tectonic burial and 'young' (< 10 Ma) exhumation in the Southern Apennines fold and thrust belt (Italy): Geology, v. 36, p. 243–246, doi:10.1130/G24344A.1.

Medwedeff, D.A., and Krantz, R.W., 2002, Kinematic and analog modeling of 3-D extensional ramps: Observations and a new 3-D deformation model: Journal of Structural Geology, v. 24, no. 4, p. 763–772, doi:10.1016/S0191-8141(01)00121-3.

Monaco, C., Bianca, M., Catalano, S., De Guidi, G., and Tortorici, L., 2002, Sudden change in the late Quaternary tectonic regime in eastern Sicily: Evidences from geological and geomorphological features: Bollettino della Società Geologica Italiana, v. 121, no. 1, p. 901–913.

Mora, O., Mallorquí, J.J., and Broquetas, A., 2003, Linear and nonlinear terrain deformation maps from a reduced set of interferometric SAR images: IEEE Transactions on Geoscience and Remote Sensing, v. 41, p. 2243–2253, doi:10.1109/TGRS.2003.814657.

Neri, G., Orecchio, B., Totaro, C., Falcone, G., and Presti, D., 2009, Subduction beneath southern Italy close the ending: Results from seismic tomography: Seismological Research Letters, v. 80, no. 1, p. 63–70, doi:10.1785/gssrl.80.1.63.

Patacca, E., Scandone, E., Giunta, G., and Liguori, V., 1979, Mesozoic paleotectonic evolution of the Ragusa zone (southeastern Sicily): Geologica Romana, v. 18, p. 331–369.

Pedley, H.M., and Grasso, M., 1991, Sea-level change around the margins of the Catania-Gela Trough and Hyblean Plateau, southeast Sicily (African-European plate convergence zone): A problem of Plio-Quaternary plate buoyancy, *in* Macdonald, D.I.M., ed., Sedimentation, Tectonics and Eustasy: Sea Level Changes at Active Margins: International Association of Sedimentologists Special Publication 12, p. 451–464.

Pedley, H.M., and Grasso, M., 1992, Miocene syntectonic sedimentation along the western margins of the Hyblean-Malta platform: A guide to plate margin processes in the central Mediterranean: Journal of Geodynamics, v. 15, no. 1–2, p. 19–37, doi:10.1016/0264-3707(92)90004-C.

Pirrotta, C., Barbano, M.S., Pantosti, D., and De Martini, P.M., 2013, Evidence of active tectonics in the Augusta Basin (eastern Sicily, Italy) by Chirp sub-bottom sonar investigation: Annals of Geophysics, v. 56, no. 5, p. S0562, doi:10.4401/ag-637.

Prati, C., Ferretti, A., and Perissin, D., 2010, Recent advances on surface ground deformation measurement by means of repeated space-borne SAR observations: Journal of Geodynamics, v. 49, p. 161–170, doi:10.1016/j.jog.2009.10.011.

Quintà, A., and Tavani, S., 2012, The foreland deformation in the south-western Basque-Cantabrian belt (Spain): Tectonophysics, v. 576–577, p. 4–19, doi:10.1016/j.tecto.2012.02.015.

Ragg, S., Grasso, M., and Müller, B., 1999, Patterns of tectonic stress in Sicily from borehole breakout observations and finite element modelling: Tectonics, v. 18, no. 4, p. 669–685, doi:10.1029/1999TC900010.

Ranero, C.R., Phipps Morgan, J., McIntosh, K., and Reichert, C., 2003, Bending-related faulting and mantle serpentinization at the Middle America Trench: Nature, v. 425, p. 367–373, doi:10.1038/nature01961.

Reuther, C.D., Ben-Avraham, Z., and Grasso, M., 1993, Origin and role of major strike slip transfers during plate collision in the central Mediterranean: Terra Nova, v. 5, p. 249–257, doi:10.1111/j.1365-3121.1993.tb00256.x.

Robertson, A.H.F., and Grasso, M., 1995, Overview of the Late Tertiary–Recent tectonic and palaeo-environmental development of the Mediterranean region: Terra Nova, v. 7, p. 114–127, doi:10.1111/j.1365-3121.1995.tb00680.x.

Ruggieri, G., and Greco, A., 1965, Studi geologici e paleontologici su Capo Milazzo con particolare riguardo al Milazziano: Geologica Romana, v. 4, p. 41–88.

Scandone, E., Patacca, E., Radoicic, R., Ryan, W.B.E., Cita, M.B., Rawson, M., Chezar, H., Miller, E., McKenzie, J., and Rossi, S., 1981, Mesozoic and Cenozoic rocks from Malta Escarpment (Central Mediterranean): American Association of Petroleum Geologists Bulletin, v. 65, p. 1299–1319.

Schmincke, H.U., Behncke, B., Grasso, M., and Raffi, S., 1997, Evolution of the northwestern Iblean Mountains, Sicily: Uplift, Pliocene/Pleistocene sea-level changes, paleoenvironment, and volcanism: Geologische Rundschau, v. 86, no. 3, p. 637–669, doi:10.1007/s005310050169.

Scicchitano, G., Antonioli, F., Berlinghieri, E.F.C., Dutton, A., and Monaco, C., 2008, Submerged archaeological sites along the Ionian coast of southeastern Sicily (Italy) and implications for the Holocene relative sea-level change: Quaternary Research, v. 70, no. 1, p. 26–39, doi:10.1016/j.yqres.2008.03.008.

Scisciani, V., Calamita, F., Tavarnelli, E., Rusciadelli, G., Ori, G.G., and Paltrinieri, W., 2001, Foreland-dipping normal faults in the inner edges of syn-orogenic basins: A case from the Central Apennines, Italy: Tectonophysics, v. 330, no. 3–4, p. 211–224, doi:10.1016/S0040-1951(00)00229-8.

Seymour, M.S., and Cumming, I.G., 1994, Maximum likelihood estimator for SAR interferometry, *in* Proceedings 1994 of the International Geoscience and Remote Sensing Symposium (IGARSS '94): Pasadena, California 1994, p. 2272–2275.

Shiner, P., Beccacini, A., and Mazzoli, S., 2004, Thin-skinned versus thick-skinned structural models for Apulian carbonate reservoirs: Constraints from the Val D'Agri Fields: Marine and Petroleum Geology, v. 21, p. 805–827, doi:10.1016/j.marpetgeo.2003.11.020.

Sinclair, H.D., 1997, Flysch to molasse transition in peripheral foreland basins: The role of the passive margin versus slab breakoff: Geology, v. 25, no. 12, p. 1123–1126, doi:10.1130/0091-7613(1997)025<1123:FTMTIP>2.3.CO;2.

Sirovich, L., and Pettenati, F., 1999, Seismotectonic outline of south-eastern Sicily: An evaluation of available options for the earthquake fault rupture scenario: Journal of Seismology, v. 3, p. 213–233, doi:10.1023/A:1009859608837.

Sowter, A., Bateson, L., Strange, P., Ambrose, K., and Syafiudin, M.F., 2013, DInSAR estimation of land motion using intermittent coherence with application to the South Derbyshire and Leicestershire coalfields: Remote Sensing Letters, v. 4, p. 979–987, doi:10.1080/2150704X.2013.823673.

Tankard, A.J., 1986, On the depositional response to thrusting and lithospheric flexure: Examples from the Appalachian and Rocky Mountain Basins, *in* Allen, P.A., and Homewood, P., eds., Foreland Basins: Oxford, UK, Blackwell Publishing Ltd., p. 369–392, doi:10.1002/9781444303810.ch20

Tarquini, S., Favalli, M., Doumaz, F., Fornaciai, A., and Nannipieri, L., 2012, Release of a 10-m-resolution DEM for the Italian territory: Comparison with global-coverage DEMs and anaglyph-mode exploration via the web: Computers & Geosciences, v. 38, p. 168–170, doi:10.1016/j.cageo.2011.04.018.

Tavani, S., Fernandez, O., and Muñoz, J.A., 2012, Stress fluctuation during thrust-related folding: Boltaña anticline (Pyrenees, Spain), *in* Healy, D., Butler, R.W.H., Shipton, Z.K., and Sibson, R.H., eds., Faulting, Fracturing, and Igneous Intrusion in the Earth's Crust: Geological Society of London Special Publication 367, p. 131–140, doi:10.1144/SP367.9.

Tavarnelli, E., and Peacock, D.C., 2002, Pre-thrusting mesoscopic extension in a syn-orogenic foredeep basin of the Umbria-Marche Apennines, Italy: Bollettino della Società Geologica Italiana, v. 121, no. 1, p. 729–737.

Tinterri, R., and Muzzi Magalhaes, P., 2011, Synsedimentary structural control on foredeep turbidites: An example from Miocene Marnoso-Arenacea Formation, Northern Apennines, Italy: Marine and Petroleum Geology, v. 28, no. 3, p. 629–657, doi:10.1016/j.marpetgeo.2010.07.007.

Turcotte, D.L., and Schubert, G., 2001, Geodynamics (2nd ed.): New York, Cambridge University Press, 472 p.

Ufficio Idrografico Regionale, 2007, Progetto Pilota per la Lotta alla Desertificazione nella Regione Sicilia: Palermo, Ufficio Idrografico Regionale, 107 p.

Vitale, S., Dati, F., Mazzoli, S., Ciarcia, S., Guerriero, V., and Iannace, A., 2012, Modes and timing of fracture network development in poly-deformed carbonate reservoir analogues, Mt. Chianello, southern Italy: Journal of Structural Geology, v. 37, p. 223–235, doi:10.1016/j.jsg.2012.01.005.

Waelbroeck, C., Labeyrie, L., Michel, E., Duplessy, J.C., Lambeck, K., McManus, J.F., Balbon, E., and Labracherie, M., 2002, Sea-level and deep water temperature changes derived from benthic foraminifera isotopic records: Quaternary Science Reviews, v. 21, p. 295–305, doi:10.1016/S0277-3791(01)00101-9.

Werner, C., Wegmüller, U., Strozzi, T., and Wiesmann, A., 2003, Interferometric point target analysis for deformation mapping, *in* Proceedings of the IEEE (Institute of Electrical and Electronic Engineers) International Geoscience and Remote Sensing Symposium (IGARSS '03), 21–25 July 2003: Toulouse, France, v. 7, p. 4362–4364.

Westaway, R., 1993, Quaternary uplift of southern Italy: Journal of Geophysical Research–Solid Earth, v. 98, no. B12, p. 21,741–21,772, doi:10.1029/93JB01566.

Whitaker, A.E., and Engelder, T., 2006, Plate-scale stress fields driving the tectonic evolution of the central Ouachita salient, Oklahoma and Arkansas: Geological Society of America Bulletin, v. 118, no. 5–6, p. 710–723, doi:10.1130/B25780.1.

Yellin-Dror, A., Grasso, M., Ben-Avraham, Z., and Tibor, G., 1997, The subsidence history of the northern Hyblean plateau margin, southeastern Sicily: Tectonophysics, v. 282, p. 277–289, doi:10.1016/S0040-1951(97)00228-X.

Zarudski, E.E.K., 1972, The Strait of Sicily—A geophysical study: Revue de Géographie Physique et de Géologie Dynamique, v. 14, p. 11–28.

Zhao, M., and Jacobi, R.D., 1997, Formation of regional cross-fold joints in the northern Appalachian Plateau: Journal of Structural Geology, v. 19, no. 6, p. 817–834, doi:10.1016/S0191-8141(97)00009-6.

MANUSCRIPT RECEIVED 4 MARCH 2015
REVISED MANUSCRIPT RECEIVED 29 MAY 2015
MANUSCRIPT ACCEPTED 15 JUNE 2015

Printed in the USA

Lithosphere, published online on 6 July 2015 as doi:10.1130/L453.1

Lithosphere

Quaternary deformation in SE Sicily: Insights into the life and cycles of forebulge fault systems

D. Di Martire, A. Ascione, D. Calcaterra, G. Pappalardo and S. Mazzoli

Lithosphere published online 6 July 2015;
doi: 10.1130/L453.1

Notes